An epsilon-constraint-based exact multi-objective optimization approach for the ship schedule recovery problem in liner shipping

Elmi, Zeinab; Li, Bokang; Liang, Benbu; Lau, Yui yip; Borowska-Stefańska, Marta; Wiśniewski, Szymon; Dulebenets, Maxim A.

DOI
10.1016/j.cie.2023.109472

Publication date
2023

Document Version
Final published version

Published in
Computers and Industrial Engineering

Citation (APA)
Elmi, Z., Li, B., Liang, B., Lau, Y. Y., Borowska-Stefańska, M., Wiśniewski, S., & Dulebenets, M. A. (2023). An epsilon-constraint-based exact multi-objective optimization approach for the ship schedule recovery problem in liner shipping. *Computers and Industrial Engineering*, *183*, Article 109472. https://doi.org/10.1016/j.cie.2023.109472

Computers & Industrial Engineering 183 (2023) 109472

Contents lists available at ScienceDirect

Computers & Industrial Engineering

journal homepage: www.elsevier.com/locate/caie

An epsilon-constraint-based exact multi-objective optimization approach for the ship schedule recovery problem in liner shipping

Zeinab Elmi [a], Bokang Li [a], Benbu Liang [b,c], Yui-yip Lau [d], Marta Borowska-Stefańska [e], Szymon Wiśniewski [e,f], Maxim A. Dulebenets [a,*]

[a] Department of Civil & Environmental Engineering, Florida A&M University-Florida State University (FAMU-FSU) College of Engineering, 2035 E Paul Dirac Dr., Sliger Building, Suite 275, Tallahassee, FL 32310, USA
[b] School of Management, Wuhan University of Technology, Wuhan 430070, China
[c] Department of Multi-Actor Systems, Faculty of Technology, Policy, and Management, Delft University of Technology, Building 31, Jaffalaan 5, 2628 BX Delft, the Netherlands
[d] Division of Business and Hospitality Management, College of Professional and Continuing Education, The Hong Kong Polytechnic University, 9 Hoi Ting Road, Yau Ma Tei, Kowloon, Hong Kong
[e] University of Lodz, Faculty of Geographical Sciences, Institute of the Built Environment and Spatial Policy, 90-142 Łódź, Kopcinskiego St. 31, Poland
[f] University of Lodz, Research Center for European Spatial Policy and Local Development, 90-142 Łódź, Kopcinskiego St. 31, Poland

ARTICLE INFO

Keywords:
Maritime supply chains
Uncertainty
Disruptions
Ship schedule recovery
Multi-objective optimization
Service reliability

ABSTRACT

Time management is crucial for liner shipping services. A variety of unexpected events can disrupt liner shipping schedules. A real-time port capacity analysis and rescheduling the original ship operations would be necessary to counteract the negative effects of such disruptions. Different ship schedule recovery options can be adopted in response to disruptive events (e.g., ship sailing speed adjustment, skipping of disrupted ports). However, shipping lines face conflicting decisions when selecting ship schedule recovery options. As an example, the commonly-used ship speeding-up option could effectively reduce delays during the voyage but would increase the fuel cost. Similarly, the skipping of disrupted ports may substantially decrease the associated delays but would incur additional costs associated with supply chain disruptions and misconnected cargo. Nevertheless, there is a lack of analytical methods that enable the evaluation of competing objectives in ship schedule recovery and effective multi-objective solution approaches. Therefore, this study proposes a novel multi-objective model for ship schedule recovery that aims not only to minimize the total late ship arrivals at ports but also to minimize the total profit loss due to disruptive events that may occur at sea and/or at ports. An epsilon-constraint-based exact optimization algorithm is adopted to obtain optimal Pareto Fronts. The computational experiments conducted for a real-life transit route demonstrate that the adopted exact optimization algorithm is able to generate Pareto Fronts in a timely manner. Moreover, the conducted sensitivity analyses provide interesting insights regarding the effects of different disruption types and unit fuel costs on ship schedule recovery.

1. Introduction

A primary mode of container transportation is maritime logistics, which enables an effective spatial distribution of containers between ports across the world (Sun et al., 2021; Ma et al., 2022; Mehrzadegan et al., 2022; Zheng et al., 2022). In 2014, shipping logistics handled a total of 9.8 billion tons of maritime trade, and the global containerized market grew by 5.3 percent to 171 million twenty-foot equivalent units (TEUs) (De et al., 2021). In 2020, 815.6 million TEUs of containers were handled in ports worldwide (UNCTAD, 2021). In recent years, containers delivered by oceangoing ships have accounted for 22% to 24% of the total ton-kilometer freight movements in the United States (McLean, 2021). In addition to the United States, Europe relies heavily on the maritime transportation system. According to the European Commission, nearly 41% of Europe's freight transit industry is carried by short-sea shipping (McLean, 2021). However, with regard to other modes of transportation services, the sea freight industry faces unprecedented and disruptive conditions, such as port closures due to labor strikes, severe

* Corresponding author.
E-mail addresses: ze20a@fsu.edu (Z. Elmi), bl22a@fsu.edu (B. Li), liangbenbu@whut.edu.cn (B. Liang), yuiyip.lau@cpce-polyu.edu.hk (Y.-y. Lau), marta.borowska@geo.uni.lodz.pl (M. Borowska-Stefańska), szymon.wisniewski@geo.uni.lodz.pl (S. Wiśniewski), mdulebenets@eng.famu.fsu.edu (M.A. Dulebenets).

https://doi.org/10.1016/j.cie.2023.109472
Received 26 November 2022; Received in revised form 21 May 2023; Accepted 21 July 2023
Available online 22 July 2023

weather conditions, and pirate attacks.

Extreme weather incidents can severely impact ships transporting cargoes. Ship arrivals at ports can be seriously hampered by bad weather, resulting in substantial financial losses and delays. For example, due to the collapse of the gantry cranes during Hurricane Matthew in 2016, the Mediterranean Shipping Company (MSC) had to divert their cargo to other ports, which delayed final deliveries by months (ICE Cargo, 2021). In November 2020, the 14,000-TEU Apus was caught in a strong storm 1,600 nautical miles northwest of Hawaii, resulting in the loss or damage of over 1,900 containers (Marle, 2022). In August 2021, Hurricane Ida, one of the costliest hurricanes in the United States history, hit the Gulf Coast, shutting down cargo operations at the Port of New Orleans for several days and causing damage to the Ports of South Louisiana and Fourchon (Kay, 2021). The Klang Port, the second largest port in Southeast Asia, was one of the areas flooded as a result of Typhoon Rai in December 2021. The flooding ceased port operations and caused major disruptions for the semiconductor supply chain, incurring losses of $28 million (Lim, 2021). Ports may be shut down as a precaution by authorities in the event of bad weather. For instance, heavy rains and destructive winds forced the closures of the Ports of Kembla, Botany, and Jackson in April 2015 in Australia. Additionally, the terminals of the Port of Shanghai (China) were shut down during Typhoon In-fa in July 2021 (ICE Cargo, 2021). Along with adverse weather events, the tidal effect may cause the depth fluctuation of berthing positions and access channels, which may further create navigational issues for oceangoing ships in the vicinity of ports (Dadashi et al., 2017; Liu et al., 2021).

The coronavirus 2019 (COVID-19) pandemic has significantly disrupted global shipping and maritime activities along established transport routes (Pasha et al., 2021; Oyenuga, 2021). Automatic Identification System (AIS) receivers recorded a decline in global shipping activities all over the world between March and June 2020, when the strictest restrictions were in effect. In March 2020, the government of Malaysia imposed restrictions on the movement of goods, resulting in high stacks of non-essential goods, especially at the Klang Port, which caused port disruptions and a slowdown in supply chain operations (Menhat et al., 2021). Countries, such as Turkey, Australia, and India, have implemented quarantine controls for ships entering the ports for 14 days, which have caused longer sailing times, disrupted sailing plans, delays in unloading cargo containers, and even shipping stoppages (Xu et al., 2021). The outbreak of COVID-19 led to an increase in the severity and frequency of port congestion events caused by various factors, putting the stability of global supply chains at risk. In November 2021, congestion at the Port of Long Beach and the Port of Los Angeles reached record highs, with up to 116 container ships either docked or anchored. In March/April 2022, the spread of the highly infectious Omicron variant in China resulted in the staggering lockdown of Shanghai, causing severe port congestion, higher freight charges, and longer cargo transit times (AGCS, 2022).

Even though liner shipping disruptions are unpredictable, it is critical that shipping lines deal with them in a timely and effective manner. An efficient disruption management strategy can give a shipping line an advantage over its competitors. In the last 20 years, operations research methods have become popular among real-time disruption management tools to ensure airline schedule execution (Clausen et al., 2010). There are apparent similarities between the airline and maritime shipping industries (Cheraghchi et al., 2017). Flying speed adjustments and flight cancellations are just some of the recovery strategies used by airlines to counteract the negative effects of disruptions (Marla et al., 2017). Certain recovery options commonly deployed in the airline industry can also be used in liner shipping to effectively address various disruptive incidents (Brouer et al., 2013). The key objective of the ship recovery problem is to make the required updates in a disrupted schedule to minimize the negative externalities caused by disruptions. Ship schedule recovery options may include a variety of measures, including but not limited to adjusting ship sailing speed during the voyage, skipping and swapping ports of call, and extending working hours at ports (Yu and Qi, 2004).

However, shipping lines face conflicting decisions when selecting ship schedule recovery options. As an example, the commonly-used ship speeding-up option could effectively reduce delays during the voyage but would increase the fuel cost. Similarly, the skipping of disrupted ports may substantially decrease the associated delays but would incur additional costs associated with supply chain disruptions and misconnected cargo. Nevertheless, there is a lack of analytical methods that enable the evaluation of competing objectives in ship schedule recovery and effective multi-objective solution approaches. Therefore, this study proposes a novel multi-objective model for ship schedule recovery that aims not only to minimize the total late ship arrivals at ports but also to minimize the total profit loss due to disruptive events that may occur at sea and/or at ports. An epsilon-constraint-based exact optimization algorithm is adopted to obtain optimal Pareto Fronts. The computational experiments conducted for the EPIC (Europe Pakistan India Consortium) shipping route demonstrate that the adopted exact optimization algorithm is able to generate Pareto Fronts in a timely manner. Moreover, the conducted sensitivity analyses provide interesting insights regarding the effects of different disruption types and unit fuel costs on ship schedule recovery.

The remaining sections of the manuscript are arranged as follows. Section 2 reviews the previously conducted studies that fall into two categories: (a) uncertainty modeling in port and liner shipping operations; and (b) recovery of ship schedules. Then, in Section 3, the multi-objective ship scheduling recovery decision problem is described in detail. A non-linear mathematical model for the considered decision problem is developed in Section 4. Section 5 presents the adopted linearization procedures and the adopted epsilon-constraint-based multi-objective optimization algorithm. Section 6 provides an in-depth description of the numerical experiments carried out as part of this study. The final section of the study mainly discusses the findings and potential directions for future research.

2. Literature review

This section focuses on the most relevant findings of the previously conducted studies in two areas: (a) studies that examine disruptions in liner shipping operations and incorporate some level of uncertainty; and (b) studies that focus on liner shipping disruptions and propose various ship schedule recovery strategies. This section also outlines the contributions of the present study to the state-of-the-art.

2.1. Review of the relevant efforts

When it comes to the design of shipping line schedules, the most common assumption in the existing liner shipping literature is that each ship will arrive within a previously scheduled fixed arrival time window at each port without considering ship scheduling uncertainties that could result in delays (Wang et al., 2014; Brouer et al., 2017; Pasha et al., 2020; Wang and Wang, 2021; Zheng et al., 2021). The study by Chuang et al. (2010) was one of the first attempts to explicitly model uncertain ship sailing time, port handling time, and container demand. The article proposed an algorithm that relied on fuzzy set theory to determine the fitness of a shipping route from its fuzzy total profit. Wang and Meng (2012a) designed a model to help liner shipping companies minimizing the overall transit cost while maintaining the required service frequency. The study modeled uncertain waiting time at ports due to potential congestion issues and uncertain time in container handling. Realistic numerical experiments validated the efficiency of the proposed iterative algorithm. Using a case study of scheduling Liquefied Natural Gas ships, Halvorsen-Weare et al. (2013) sought to design schedules that were resilient to weather changes.

Du et al. (2015) created a fuel budgeting optimization model that directly captured potential severe weather conditions. The

mathematical model was solved using the polynomial-time method. Tierney et al. (2019) analyzed ship transit time data to create three mathematical models focusing on the following aspects: design sailing speed, optimum sailing speed, and optimized speed with maximum travel time. The study utilized buffer time to meet the expected customer level of service. Liu et al. (2020) developed a non-linear speed and bunkering optimization model under uncertain container demand. Piecewise linear functions were used to approximate bunker consumption and simplify the non-linear model. The L-shape algorithm used to solve the model was efficient in terms of both computational time and quality of produced solutions. Ding and Xie (2022) proposed a two-stage non-linear mathematical model with schedule-sensitive demand and stochastic shipment times. The model was linearized by adding nominal delay variables. The Bender's decomposition algorithm was deployed for the linearized problem.

All the aforementioned studies modeled liner shipping scheduling uncertainty without introducing any recovery options to offset the effects of disruptive incidents. Another relevant group of studies investigated the various liner shipping schedule recovery options that can mitigate negative effects of disruptive incidents. Paul and Maloni (2010) analyzed the impact of various port network disruptions. A real-time assessment was conducted to conform to dynamic port services. The network's overall capacity was optimized to reduce port and inventory costs. Jones et al. (2011) designed a modeling tool to simulate import/export container movements in the United States under a variety of disruptive scenarios, such as security check delays and port disruptions. The model's objective was to reduce the overall shipping costs. The method was found to be effective and could be used by a variety of stakeholders as a planning tool. Brouer et al. (2013) proposed an NP-hard model for ship schedule recovery. The model's performance was evaluated on four real-world instances using the CPLEX solver and a variety of recovery methods. The proposed model provided comparable or better solutions than real-world recovery options. Li et al. (2015) developed an operational ship schedule recovery strategy that accounts for uncertainties. For long delays, the swapping of ports and the skipping of ports were considered as recovery approaches, while speed adjustment was considered for minor disruptions.

Qi (2015) provided an overview of disruption and uncertainty management in liner ship schedules. A single-ship recovery model and a multi-ship recovery model were developed to minimize the costs associated with bunker consumption and late ship arrivals. A dynamic programming-based solution method was presented to solve the proposed models. Li et al. (2016) proposed a ship schedule recovery model that considers both regular and irregular disruptive incidents. The recovery model was designed as a stochastic optimization formulation to minimize the cost related to the delayed arrival time and bunker consumption. An optimal control policy was discovered through the backward value iteration. As discussed earlier, some of liner shipping decisions are inherently conflicting. To analyze the contradictory relationships between objectives in liner ship scheduling, Cheraghchi et al. (2017), Cheraghchi et al. (2018), and Cheraghchi et al. (2020) proposed multi-objective models for simultaneously optimizing the competing objectives (i.e., minimization of total financial losses, minimization of total delays, and maximization of average speed compliance). Sailing speed adjustment was considered as the primary recovery option.

Abioye et al. (2019) created a mathematical model to minimize ship financial losses for routes passing via emission control zones. The study considered ship speeding-up and skipping of disrupted ports as the main recovery options. The proposed method was found to be both energy-efficient and sustainable while also reducing the total monetary loss. Mulder and Dekker (2019) proposed a model to optimize ship schedule recovery by incorporating buffer time. The study used mixed-integer programming and Markov decision processes. Four heuristics were proposed to deal with the problem's runtime restrictions and the curse of dimensionality. A 28.9 percent reduction in costs was achieved by optimizing buffer time. Mulder et al. (2019) created a method to plan and implement ship timetables. A stochastic dynamic program was used to model the execution of the timetable. The optimized timetable would save $4 to $10 million per route per year. Xing and Wang (2019) were the first to consider both the ship schedule recovery model and container flow recovery plan to balance schedule recovery and service costs. A total of three schedule recovery tiers were considered: shortening port and sea time, swapping port call orders, and omitting a call. The priority of the tiers for recovery options decreased sequentially based on the severity of the penalties.

Abioye et al. (2021) presented a ship schedule recovery problem that took into account various recovery actions and disruptive incidents. The proposed non-linear ship scheduling model was solved using the BARON optimization solver. De et al. (2021) considered ship rerouting and port swapping as the primary recovery options to address weather-related delays. The effects of fuel prices and carbon taxes on the overall operating costs of shipping were investigated. The study provided shipping companies with alternative ship route options for normal or disrupted scenarios. Asghari et al. (2022) presented an optimization model for ship schedule recovery, considering sailing speed adjustment and port skipping as the primary recovery options. A Crowd-Learning Particle Swarm Optimization Algorithm was used as a solution approach. Real-life scenarios of disruptive incidents were investigated as a part of the study, which showed the effectiveness of the proposed solution methodology. Du et al. (2022a) proposed a machine learning-based approach under sailing and port time uncertainty. A machine learning method relied on speed optimization, neural network training, and reinforcement learning. A set of numerical studies showed that the proposed machine learning-based approach effectively optimized ship schedules.

2.2. Literature summary, critical gaps, and contributions of this work

Table 1 provides a summary of the evaluated studies, including the following information: the author(s), year of publication, study category, model's objective, solution technique, important notes and major considerations incorporated by the reviewed studies. The conducted literature review shows that the minimization of the overall shipping cost was the most popular objective among the existing studies on liner shipping uncertainties and ship schedule recovery.

Furthermore, a very limited number of studies proposed multi-objective mathematical formulations that can be used to capture the competing objectives in ship schedule recovery (Cheraghchi et al., 2017; Cheraghchi et al., 2018; Cheraghchi et al., 2020; Elmi et al., 2022). However, the proposed multi-objective mathematical models mainly consider the adjustment of ship sailing speed as the only recovery option to offset the negative impacts of disruptive incidents. Moreover, different metaheuristic algorithms were mostly used for multi-objective ship schedule recovery models (Cheraghchi et al., 2017; Cheraghchi et al., 2018; Cheraghchi et al., 2020; Elmi et al., 2022). Although multi-objective metaheuristic algorithms normally show competitive performance in terms of computational time for large-scale problems, they do not guarantee optimality of the obtained Pareto Fronts. Considering these shortcomings in the state-of-the-art, the present study offers the following main contributions:

Table 1
Review summary for the most relevant studies.

a/a	Authors	Year	Category	Objective(s)	Solution Technique	Important Notes and Major Considerations
1	Chuang et al.	2010	USSP	Maximize the overall profit	Metaheuristic	Developing a fuzzy Genetic Algorithm for liner shipping scheduling
2	Paul and Maloni	2010	SSRP	Minimize the overall shipping cost	Heuristic	Modeling disruptive incidents at ports
3	Jones et al.	2011	SSRP	Minimize the overall shipping cost	Heuristic	Simulating disruptive incidents for the United States freight intermodal network via a decision support tool
4	Wang and Meng	2012	USSP	Minimize the overall shipping cost	Iterative method	Buffer time at voyage legs
5	Brouer et al.	2013	SSRP	Minimize the overall shipping cost	CPLEX	Evaluated the complexity of the ship schedule recovery model
6	Halvorsen-Weare et al.	2013	USSP	Minimize the overall shipping cost	Xpress-IVE	Considered the possible effects of weather changes
7	Du et al.	2015	USSP	Minimize the overall fuel consumption	Iterative method	Adverse weather effects on the total fuel consumption
8	Li et al.	2015	SSRP	Minimize the overall shipping cost	DP	Identifying an appropriate delay penalty function
9	Qi	2015	SSRP	Minimize the overall shipping cost	DP	Single-ship and multiple-ship models for the real-time ship schedule recovery problem
10	Li et al.	2016	SSRP	Minimize the overall shipping cost	DP	Distinguishing various regular uncertainties and disruptive incidents
11	Cheraghchi et al.	2017	SSRP	Maximize the average speed compliance; Minimize the monetary loss; Minimize the overall delay	Metaheuristics	Application of the AIS data to assess ship schedule delays
12	Cheraghchi et al.	2018	SSRP	Minimize the monetary loss; Minimize the overall delay	Metaheuristic	Evaluation of voyage distances, problem scalability, and ship steaming policies
13	Abioye et al.	2019	SSRP	Minimize the overall monetary loss	CPLEX	Considering the regulatory enforcement within emission control zones
14	Mulder and Dekker	2019	SSRP	Minimize the overall shipping cost	Heuristics	Allocation of buffer times
15	Mulder et al.	2019	SSRP	Minimize the overall shipping cost	Iterative method	Execution of a timetable with stochastic delays
16	Tierney et al.	2019	USSP	Minimize the overall shipping cost	GUROBI	The liner shipping transit time was based on empirical data
17	Xing and Wang	2019	SSRP	Minimize the overall shipping cost	LINGO	Consideration of the container flow recovery problem with ship schedule recovery
18	Cheraghchi et al.	2020	SSRP	Maximize the average speed compliance; Minimize the monetary loss; Minimize the overall delay	Metaheuristics	Development of a model for multi-objective optimization using the AIS data
19	Liu et al.	2020	USSP	Minimize the overall shipping cost	Iterative method	Optimizing the bunkering and speed of liner ships
20	Abioye et al.	2021	SSRP	Minimize the monetary loss	BARON	Examining various real-world disruption scenarios and recovery options
21	De et al.	2021	SSRP	Maximize the overall profit	Heuristic	Incorporated the effects of fuel prices and carbon taxes
22	Asghari et al.	2022	SSRP	Minimize the overall shipping cost	Metaheuristics	Consideration of emission charges in the proposed model
23	Ding and Xie	2022	USSP	Maximize the overall profit	Iterative method	Managing the risk of unexpected delays while adhering to tight deadlines
24	Du et al.	2022a	SSRP	Minimize the overall shipping cost	Heuristic	A machine learning-based solution for liner shipping optimization

Used Abbreviations: Category [USSP – uncertainties in the ship scheduling problem; SSRP – the ship schedule recovery problem]; Solution Technique [BARON – optimization solver; CPLEX – optimization solver; DP – Dynamic Programming; GUROBI – optimization solver; LINGO – optimization solver; Xpress-IVE – optimization solver]; Important Notes and Major Considerations [AIS – Automatic Identification System].

- A new optimization model is developed for ship schedule recovery to effectively offset the effects of disruptive incidents in liner shipping.
- A variety of recovery options are proposed within the multi-objective framework, including port skipping, port skipping with the diversion of containers, increasing ship sailing speeds at specific voyage legs, and increasing ship handling rates at specific ports.
- An epsilon-constraint-based exact optimization algorithm is adopted to obtain optimal Pareto Fronts in a timely manner.
- A set of extensive experiments are conducted for a real-life shipping route to evaluate the performance of the proposed algorithm and ship schedule recovery options.
- The conducted sensitivity analyses provide interesting insights regarding the effects of different disruption types and unit fuel costs on ship schedule recovery.

3. Problem Description

3.1. Description of liner shipping transit routes

Sea routes connecting multiple ports are primarily served by a single shipping line (a.k.a., liner shipping company) or an alliance. This research will focus on modeling shipping routes serviced by a single shipping company. A liner shipping route consists of several ports, which will be denoted as $P = \{1, \cdots, n\}$. Ships visit each port once or several times during a voyage. In the liner shipping literature, the sequence of ports to be called is known as "port rotation". A port rotation generally differs from one route to another. The itineraries of the deployed ships and service frequency are determined in the strategic and tactical planning levels (Meng et al., 2014; Dulebenets et al., 2021). Fig. 1 shows an example liner shipping transit route of a liner shipping company passing through 7 ports of call. The port rotation starts from port "1". Port "3" will be visited twice, while the other ports will be visited once. A "voyage leg" refers the distance traveled by a ship between two subsequent ports on the same route. Every ship allocated for service of the given port rotation travels along voyage leg p from port p to port $p + 1$. At ports along the transit route, import containers are offloaded from ships, and export containers are loaded onto ships. Upon completion of service at the last port of call, each ship sails back to the port of origin.

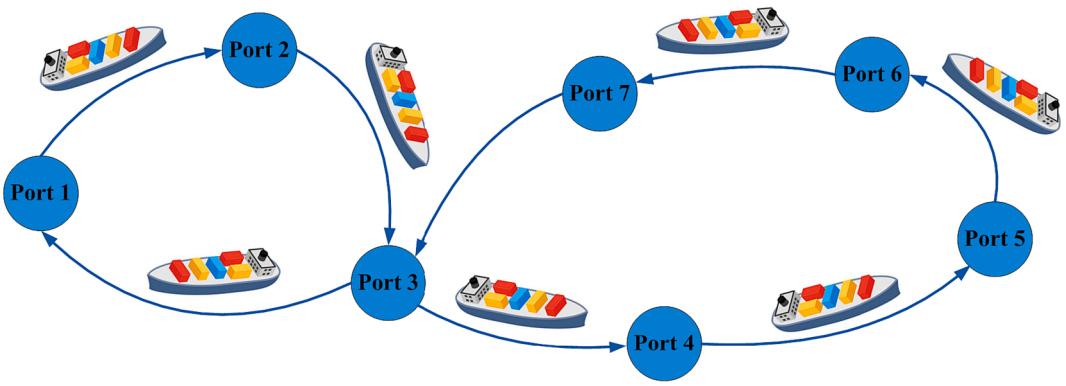

Fig. 1. Example liner shipping transit route.

3.2. Service of ships at ports

The port arrival time windows (TWs) at each port of call are defined by the port operators and liner shipping companies in the tactical level of liner shipping planning (Pasha et al., 2021). Planned port arrival TWs are specified by the following two components: (1) $\tau_p^{st}, p \in P$ (hours) represents the negotiated start of TW at port p; and (2) $\tau_p^{end}, p \in P$ (hours) denotes the negotiated end of TW at port p. If a ship arrives before the expected arrival TW, it normally waits for service at the waiting area located near the port. The waiting time ($\tau_p^{wait}, p \in P$ – hours) at ports can be obtained from the following formulas:

$$\tau_{p+1}^{wait} = \tau_{p+1}^{st} - \left(\tau_p^{dep} + \tau_p^{sail}\right) \forall p \in P, p < n \tag{3.1}$$

$$\tau_1^{wait} = \tau_1^{st} - \left(\tau_p^{dep} + \tau_p^{sail}\right) + \varphi \bullet V \forall p \in P, p = n \tag{3.2}$$

where: $\tau_{p+1}^{st}, p \in P$ – negotiated arrival TW start at port $p+1$ (hours); τ_1^{st} – negotiated arrival TW start at port "1" (hours); $\tau_p^{dep}, p \in P$ – planned ship departure time from port p (hours); $\tau_p^{sail}, p \in P$ – planned ship sailing time at voyage leg p (hours); φ – original negotiated service frequency of ports (hours); and V – number of allocated ships (ships).

The total turnaround time is the additional term ($\varphi \bullet V$) included on the right side of the waiting time formula. The total turnaround time represents the time required by the ships to visit all of the ports on the particular liner shipping transit route and return to the starting port (Abioye et al., 2019; Pasha et al., 2021). However, disruptions during the ship voyage can increase the planned total turnaround time of ships. Following the agreements between liner shipping companies and port operators, port operators are able to provide a set of container handling rates $H_p = \{1, \cdots, m_p\}, p \in P$ for ship service. The planned handling time ($\tau_p^{hand}, p \in P$ – hours) at port p can be obtained based on the original container demand ($d_p^{port}, p \in P$ – TEUs) and handling productivity (pr_{ph}, $p \in P, h \in H_p$ – TEUs/hour) as follows:

$$\tau_p^{hand} = \sum_{h \in H_p} \left(\frac{d_p^{port}}{pr_{ph}}\right) x_{ph} \forall p \in P \tag{3.3}$$

where: $x_{ph}, p \in P, h \in H_p$ – the parameter adopted to specify if container handling rate h is chosen at port p (=1) or else (=0).

It should be noted that a handling rate with higher handling productivity reduces the ship handling time but increases the port handling cost incurred by the shipping line. The unit handling cost ($c_{ph}^{port}, p \in P, h \in H_p$ – USD/TEU) will be calculated based on the requested handling rate at port p. Disruptive events (such as labor strikes, bad weather, port congestion, and even port closure) that mainly happen at ports cannot be foreseen in the tactical level and may cause severe delays in expected waiting time and handling time at ports (Li et al. 2015). Furthermore, delays due to disruptions at a given port of call may spread across the voyage, affecting the ship arrival times at subsequent ports. The delayed arrival time of ships at port p ($\overline{\tau_p^{del}}, p \in P$ – hours) can be obtained using the following formula:

$$\overline{\tau_p^{del}} \geq \overline{\tau_p^{arr}} - \tau_p^{arr} \forall p \in P \tag{3.4}$$

where: $\overline{\tau_p^{arr}}, p \in P$ – ship arrival time at port p for the recovered schedule after the occurrence of disruptive incidents (hours); $\tau_p^{arr}, p \in P$ – original planned ship arrival time at port p (hours).

3.3. Ship sailing speed and fuel consumption modeling

One of the primary premises of this study is the homogeneous nature of the ships assigned for service on the shipping line's transit route (Wang et al., 2014; Abioye et al., 2019). It means that all ships in the fleet serving a specific liner shipping route have the same technical specifications, including the structure of the engines, engine capacity, maximum sailing speed, etc. Throughout the tactical level planning, the liner shipping companies set the sailing speed of ships ($s_p, p \in P$ – knots) at each transit leg of the voyage (Pasha et al., 2021). If disruptive incidents happen when ships sail at sea, the sailing speed might be reduced at particular voyage legs (e.g., sailing speed reduction due to a severe storm at sea). Thus, the sailing speed for the recovered ship schedule or "recovered ship sailing speed" ($\overline{s_p}, p \in P$ – knots) might be lower than the sailing speed that was planned at the tactical level ($\overline{s_p} < s_p, p \in P$). In order to offset the delays caused by disruptions, the shipping line may decide to increase the sailing speed at certain transit legs, and, hence, the recovered ship sailing speed would be higher than the planned ship sailing speed at the transit legs after the implementation of sailing speed adjustment. However, for the scenarios with high unit fuel prices, the shipping line may decide to endure the delay and do not use the sailing speed adjustment strategy to prevent high fuel costs. Furthermore, the recovered ship sailing speed is directly associated with the sailing speed upper and lower bounds. The upper bound on ship sailing speed (s^{max} – knots) is imposed by the power of the ship main engine (Pasha et al., 2021). Moreover, the lower bound (s^{min} – knots) should be satisfied to prevent the wear of the ship main engine (Pasha et al., 2021). Based on the available literature (Kontovas, 2014; Zhao et al., 2019; Pasha et al., 2021), the following formula will be adopted to obtain the bunker fuel consumption at leg p ($\overline{f_p}, p \in P$ – tons/nmi) considering the recovered ship sailing speed and ship payload:

$$\overline{f_p} = \frac{\gamma(\overline{s_p})^{(\alpha-1)}}{24} \bullet \left(\frac{d_p^{sea} \bullet AWT + LWT}{TWT + LWT}\right)^{2/3} \forall p \in P \tag{3.5}$$

where: α, γ – coefficients of the fuel consumption function; d_p^{sea} – number of containers on board the ship at voyage leg p (TEUs); AWT – standardized 20-foot container cargo weight (tons); LWT – total ship

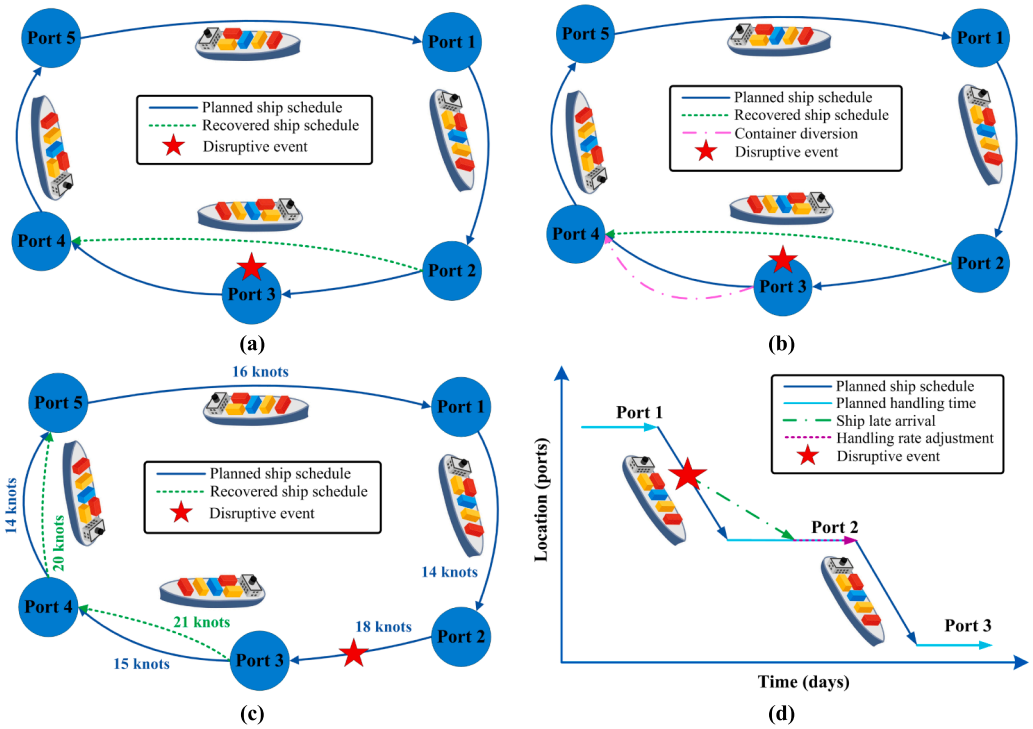

Fig. 2. Recovery options: (a) port skipping; (b) port skipping with the diversion of containers; (c) ship sailing speed adjustment at sea; and (d) handling rate adjustment at ports.

empty weight (tons); and *TWT* – total ship maximum allowable container weight (tons).

Note that the bunker fuel consumption function coefficients are generally derived based on the daily bunker fuel consumption information collected from different ships. The power adjustment "$(\alpha - 1)$" and coefficient "24" in the denominator of equation (3.5) are used to convert the bunker fuel consumption from tons per day to tons per nautical mile (Wang and Meng, 2012b). Furthermore, the power of "2/3" is used to capture the changes in bunker fuel consumption due to the changes in ship payload (Kontovas, 2014).

3.4. Disruptions and ship schedule recovery

This study proposes four primary options shipping lines can employ to compensate for the time losses due to disruptive incidents throughout the ship voyage. These recovery options include: (1) port skipping without the diversion of containers to alternative ports; (2) port skipping with the diversion of containers to alternative ports; (3) increasing ship sailing speeds at specific voyage legs; and (4) increasing ship handling rates at specific ports. The shipping line may elect to tolerate the delays caused by disruptive incidents. However, if these delays last for a significant amount of time at a particular port, the shipping line might decide to bypass that port. Skipping ports could help liner shipping companies to reduce the extra cost induced by disruptive incidents. When ships bypass a port because of unforeseen disruptive incidents, a port skipping cost should be paid to the port operators to compensate for the cost of allocated yard storage space, reserved handling equipment, and unsatisfied demand. In addition, skipping a port prevents the designated import and export cargoes from being delivered or picked up, respectively. Fig. 2**(a)** illustrates an example of a recovery option, where port "3" experienced a disruptive incident, and the shipping line decided to skip that port.

The unsatisfied demand due to port skipping could be diverted to other ports and transported via alternative inland modes to ensure the shipments arrive at their final destinations. In that case, there will be an extra cost (e.g., container handling and transporting costs at an alternative port) that the shipping line should cover. Fig. 2**(b)** depicts a scenario, in which a ship was supposed to stop at five different ports ("1", "2", "3", "4", and "5"), but the shipping line decided to bypass port "3" due to a disruptive incident at that port. Moreover, the export cargoes that were planned to be loaded on board the ship at port "3" were diverted to port "4", where the available handling equipment could be further used to complete the export container loading process. In the meantime, the import containers that were planned to be unloaded at port "3" could be unloaded at alternative port "4". The intermodal connections of port "4" could be further used to transport the shipments to their final destinations. The options of port skipping with and without the diversion of containers to alternative ports are viewed as effective to compensate for substantial time losses due to large-scale disruptive incidents (Elmi et al., 2022).

Another recovery option for the shipping line is to increase the sailing speed of ships along the voyage legs during the journey to get back on schedule and maintain the same arrival time at each subsequent port. It is assumed in this research that adjusting the transit speed could not be applied by the shipping line for the ship sailing along the voyage leg that experiences a disruptive incident. An illustration of a ship speed adjustment recovery option is shown in Fig. 2**(c)**. In this example, the shipping schedule was disrupted at sea along voyage leg "2" that connects ports "2" and "3". The shipping company decided to speed up the ships sailing along voyage legs "3" and "4" to get back on schedule. In particular, the ship sailing speed was increased from the original speed of 15 knots at voyage leg "3" to 21 knots. Furthermore, the ship sailing speed was increased from the original speed of 14 knots at voyage leg "4" to 20 knots.

At the tactical level of liner shipping planning, the handling rates are negotiated by a given shipping line with port operators at each port of call (Meng et al., 2014; Dulebenets et al., 2021). It is assumed that the shipping line can also request certain port operators (i.e., the ones that have available handling equipment) to provide a higher handling rate for ship service at a given port in order to offset the delays incurred throughout the voyage at the operational level. Higher handling rates correspond to higher productivity and faster service at ports. The

decision variable for handling rate selection at ports can be denoted as $\overline{x_{ph}}, p \in P, h \in H_p$ (=1 if h is the requested handling rate at port p; else = 0). If a shipping line requests a higher handling rate, proportionally higher port handling costs will be applied. Equation (3.6) can be used to obtain the recovered ship handling time at port p ($\overline{\tau_p^{hand}}, p \in P$ – hours) based on the actual container demand for the recovered ship schedule ($\overline{d_p^{port}}, p \in P$ – TEUs) and handling productivity ($pr_{ph}, p \in P, h \in H_p$ – TEUs/hour):

$$\overline{\tau_p^{hand}} = \sum_{h \in H_p} \left(\frac{\overline{d_p^{port}}}{pr_{ph}} \right) \overline{x_{ph}} \; \forall p \in P \tag{3.6}$$

Fig. 2**(d)** shows an example of implementing the handling rate adjustment recovery option, where the disruptive incident happened when the ship was sailing between ports "1" and "2". The ship arrival at port "2" was delayed, so the shipping line requested a higher handling rate at port "2". The implementation of the handling rate adjustment recovery option at port "2" enabled the ship leaving port "2" in a timely manner and sailing to port "3" based on the planned schedule. The options of ship sailing speed adjustment at sea and handling rate adjustment at ports are viewed as effective to compensate for small to moderate time losses due to small- and medium-scale disruptive incidents (Elmi et al., 2022). The shipping line may employ any of the proposed recovery options to restore the ship original schedule. Depending on the nature of disruptive incidents and their consequences, the shipping line may decide to apply several various recovery options throughout the voyage. However, if the shipping company determines that the price of implementing multiple recovery options (or even one recovery option) is too high, it may opt to bear the costs associated with the consequences of the disruption without using any recovery options.

3.5. Container inventory throughout ship voyage

A ship that bypasses a port due to the disruption would be unable to deliver the associated import containers and/or collect the associated export containers. However, if a shipping line decides to divert the containers to alternative ports that have an inland connection with the skipped port, the import and export container shipments can be handled accordingly. In particular, the export containers could be delivered from the skipped port via the inland connection and then loaded on board the ship at an alternative port. Furthermore, the import containers that were originally scheduled to be offloaded at the skipped port can be offloaded at an alternative port, and the intermodal connections of the alternative port could be used for the delivery of container shipments to their final destinations. Therefore, port skipping and container diversion decisions directly affect the total number of containers to be transported by the ships throughout their voyage and, hence, the overall container inventory.

A detailed example of port skipping and container diversion operations is provided in Fig. 3. In the considered example, the port rotation has five ports of call, and port "3" experienced a disruptive event. The shipping line decided to skip port "3" and divert the associated cargo to port "4", which has an inland connection with port "3". Therefore, the container demand of 400 TEUs from port "3" with 60% of import containers and 40% of export containers ($d_3^{port} = 400$ TEUs, $IMP_3 = 60\%$) was handled at port "4". Since no import containers were unloaded and no export containers were loaded at port "3", the number of containers on board the ship at voyage leg "3" connecting ports "3" and "4" was the same as the number of containers on board the ship at voyage leg "2" connecting ports "2" and "3" (i.e., $d_2^{sea} = d_3^{sea} = 6,000$ TEUs). The container demand of 800 TEUs at port "4" with 40% of import containers and 60% of export containers was handled upon arrival of the ship at port "4". The number of containers on board the ship at voyage leg "4" connecting ports "4" and "5" can be estimated based on the

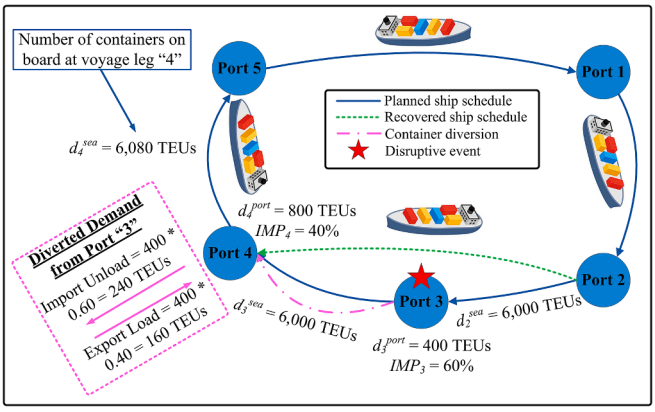

Fig. 3. An example of port skipping and container diversion operations.

number of containers on board the ship at voyage leg "3", the number of import containers that were unloaded at port "4" (i.e., $800 \bullet 0.40 = 320$ TEUs), the number of export containers that were loaded at port "4" (i.e., $800 \bullet 0.60 = 480$ TEUs), the number of import containers diverted for unloading at port "4" from port "3" that experienced a disruption (i.e., $400 \bullet 0.60 = 240$ TEUs), and the number of export containers diverted for loading at port "4" from port "3" that experienced a disruption (i.e., $400 \bullet 0.40 = 160$ TEUs) as follows: $d_4^{sea} = 6,000 - (800 \bullet 0.40 - 800 \bullet 0.60) - (400 \bullet 0.60) + (400 \bullet 0.40) = 6,080$ TEUs.

Based on the considered example, the total number of containers to be transported by the ship at voyage leg $p^* + 1$ for the recovered ship schedule ($d_{(p^*+1)}^{sea}, p^* \in P$ – TEUs) can be obtained based on the total number of containers to be transported by the ship at voyage leg p^* ($d_{p^*}^{sea}, p^* \in P$ – TEUs), the number of import containers $[d_{(p^*+1)}^{port} \bullet IMP_{(p^*+1)}, p^* \in P$ – TEUs] and export containers $[d_{(p^*+1)}^{port} \bullet (1 - IMP_{(p^*+1)}), p^* \in P$ – TEUs] handled at port $p^* + 1$, the number of import containers diverted for unloading at port $p^* + 1$ from the alternative ports that experienced a disruption $[d_{p(p^*+1)}^{div} \bullet IMP_p, p, p^* \in P, p \neq p^*$ – TEUs], and the number of export containers diverted for loading at port $p^* + 1$ from the alternative ports that experienced a disruption $[d_{p(p^*+1)}^{div} \bullet (1 - IMP_p), p, p^* \in P, p \neq p^*$ – TEUs] using the following formulas:

$$\begin{aligned} d_{(p^*+1)}^{sea} = d_{p^*}^{sea} - \Big[& d_{(p^*+1)}^{port} \bullet IMP_{(p^*+1)} - d_{(p^*+1)}^{port} \bullet \left(1 - IMP_{(p^*+1)}\right) \Big] \\ & \bullet \left(1 - x_{(p^*+1)}^{skip}\right) - \sum_{p \in P: p \neq (p^*+1)} d_{p(p^*+1)}^{div} \bullet IMP_p + \sum_{p \in P: p \neq (p^*+1)} d_{p(p^*+1)}^{div} \\ & \bullet \left(1 - IMP_p\right) \forall p^* \in P, p^* < n \end{aligned} \tag{3.7}$$

$$\begin{aligned} d_{(1)}^{sea} = d^{sea-0} - \Big[& d_{(1)}^{port} \bullet IMP_{(1)} - d_{(1)}^{port} \bullet \left(1 - IMP_{(1)}\right) \Big] \\ & \bullet \left(1 - x_{(1)}^{skip}\right) - \sum_{p \in P: p \neq (1)} d_{p(1)}^{div} \bullet IMP_p + \sum_{p \in P: p \neq (1)} d_{p(1)}^{div} \bullet \left(1 - IMP_p\right) \end{aligned} \tag{3.8}$$

where: $d_p^{port}, p \in P$ – original container demand at port p (TEUs); IMP_p, $p \in P$ – planned percentage of unloaded import containers from a ship at port p (%); $x_p^{skip} = 1$ if disrupted port p will be skipped (else = 0); $d_{pp^*}^{div}, \forall p, p^* \in P, p \neq p^*$ – number of diverted containers from disrupted port p to alternative port p^* (TEUs); and d^{sea-0} – total number of containers on board the ship prior to docking at its first port (TEUs).

When the shipping line makes container diversion decisions, it is necessary to keep in mind that the total number of containers on board the ships should not exceed their capacity. Such operational condition can be satisfied by imposing the following constraint set:

$$d_p^{sea} \bullet AWT \leq TWT \forall p \in P \tag{3.9}$$

where: AWT – standardized 20-foot container cargo weight (tons); and TWT – total ship maximum allowable container weight (tons).

3.6. Competing objectives

One of the primary objectives in ship schedule recovery is to minimize the total delays due to the occurrence of disruptive incidents throughout the voyage. The minimization of delays would assist the shipping line with maintaining an acceptable level of service for the existing customers and have their shipments delivered with the least delays possible. As discussed earlier, a variety of recovery options could be implemented by the shipping line to reduce or completely eliminate the delays due to the occurrence of disruptive incidents, including port skipping without the diversion of containers to alternative ports, port skipping with the diversion of containers to alternative ports, increasing ship sailing speeds at specific voyage legs, and increasing ship handling rates at specific ports. However, the shipping line will incur additional costs in order to implement any of the aforementioned recovery options. In particular, in case of port skipping, the shipping line will have to compensate the operator of the skipped port for the reserved handling equipment. Moreover, the costs associated with misconnected cargo will be applied as well. In case the shipping line decides to implement port skipping with the diversion of containers to alternative ports, the additional costs will be incurred for the handling of the diverted cargo at alternative ports and the inland transport of the shipments to their final destinations. The sailing speed adjustment option will increase the fuel consumption cost, whereas the handling rate adjustment option will increase the container handling costs at ports. The tradeoffs among the competing objectives should be carefully analyzed by the shipping line when planning multi-objective ship schedule recovery.

4. Multi-Objective mathematical formulation

In this part of the manuscript, the notations used for the mathematical formulation of the multi-objective ship schedule recovery problem in the present study are explained in detail, along with the formulation itself.

4.1. Adopted notations

4.1.1. Sets

Sets	Definition of Sets
$P = \{1, \cdots, n\}$	set of port visits for the specific liner shipping route (port visits)
$H_p = \{1, \cdots, m_p\}, p \in P$	set of available port handling rates at port p (port handling rates)

4.1.2. Decision variables

Decision Variables	Description of Decision Variables
$\Delta_p^{sea} \in \mathbb{R} \forall p \in P$	sailing speed adjustment of a ship at voyage leg p (knots)
$x_{ph} \in \mathbb{B} \forall p \in P, h \in H_p$	=1 if port handling rate h will be chosen at port p (else = 0)
$x_p^{skip} \in \mathbb{B} \forall p \in P$	=1 if disrupted port p will be skipped (else = 0)
$x_{pp^*}^{div} \in \mathbb{B} \forall p, p^* \in P, p \neq p^*$	=1 if there is a container diversion from disrupted port p to port p^* (else = 0)

4.1.3. Auxiliary variables

Auxiliary Variables	Description of Auxiliary Variables
$\overline{\tau_p^{arr}} \in \mathbb{R}^+ \forall p \in P$	recovered ship arrival time at port p (hours)
$\overline{\tau_p^{wait}} \in \mathbb{R}^+ \forall p \in P$	recovered ship waiting time at port p (hours)
$\overline{\tau_p^{hand}} \in \mathbb{R}^+ \forall p \in P$	recovered ship handling time at port p (hours)

(continued on next column)

(continued)

Auxiliary Variables	Description of Auxiliary Variables
$\overline{\tau_p^{dep}} \in \mathbb{R}^+ \forall p \in P$	recovered ship departure time from port p (hours)
$\overline{s_p} \in \mathbb{R}^+ \forall p \in P$	recovered ship sailing speed at voyage leg p (knots)
$\overline{\tau_p^{sail}} \in \mathbb{R}^+ \forall p \in P$	recovered ship sailing time at voyage leg p (hours)
$\overline{\tau_p^{del}} \in \mathbb{R}^+ \forall p \in P$	recovered ship delayed arrival time at port p (hours)
$\overline{STT} \in \mathbb{R}^+$	recovered ship total turnaround time of the considered shipping route (hours)
$\overline{f_p} \in \mathbb{R}^+ \forall p \in P$	recovered fuel consumption by ship main engines at voyage leg p (tons/nmi)
$d_p^{sea} \in \mathbb{R}^+ \forall p \in P$	number of containers on board the ship at voyage leg p (TEUs)
$\overline{d_p^{port}} \in \mathbb{R}^+ \forall p \in P$	recovered container demand at port p (TEUs)
$x_p^{dd} \in \mathbb{B} \forall p \in P$	=1 if the diverted containers from a disrupted port will be serviced at alternative port p (else = 0)
$d_{pp^*}^{div} \in \mathbb{N} \forall p, p^* \in P, p \neq p^*$	number of diverted containers from disrupted port p to alternative port p^* (TEUs)
$\overline{FCC} \in \mathbb{R}^+$	total recovered fuel consumption cost (USD)
$\overline{TPC} \in \mathbb{R}^+$	total recovered handling operations cost at ports (USD)
$\overline{CDC} \in \mathbb{R}^+$	total recovered container diversion cost (USD)
$\overline{REV} \in \mathbb{R}^+$	total recovered revenue obtained by the shipping line (USD)

4.1.4. Parameters

Parameters	Description of Parameters
$n \in \mathbb{N}$	number of ports to be visited for the specific liner shipping route (port visits)
$m_p \in \mathbb{N} \forall p \in P$	number of handling rates that a shipping line can request at port p (port handling rates)
$d_p^{port} \in \mathbb{R}^+ \forall p \in P$	original container demand at port p (TEUs)
$IMP_p \in \mathbb{R}^+ \forall p \in P$	planned percentage of unloaded import containers from a ship at port p (%)
$\tau_p^{st} \in \mathbb{R}^+ \forall p \in P$	negotiated arrival time window start at port p (hours)
$\tau_p^{arr} \in \mathbb{R}^+ \forall p \in P$	original planned ship arrival time at port p (hours)
$pr_{ph} \in \mathbb{R}^+ \forall p \in P, h \in H_p$	container handling productivity with handling rate h at port p (TEU/hour)
$\varphi \in \mathbb{R}^+$	original negotiated service frequency of ports (hours)
$V \in \mathbb{N}$	number of allocated ships (ships)
$d_p^{leg} \in \mathbb{R}^+ \forall p \in P$	length of voyage leg p (nmi)
$\alpha, \gamma \in \mathbb{R}^+$	fuel consumption function coefficients
$AWT \in \mathbb{R}^+$	standardized 20-foot container cargo weight (tons)
$LWT \in \mathbb{R}^+$	total ship empty weight (tons)
$TWT \in \mathbb{R}^+$	total ship maximum allowable container weight (tons)
d^{sea-0}	total number of containers on board the ship prior to docking at its first port (TEUs)
$s^{max} \in \mathbb{R}^+$	maximum allowed speed for ships (knots)
$s^{min} \in \mathbb{R}^+$	minimum allowed speed for ships (knots)
$s_p \in \mathbb{R}^+$	sailing speed of ships according to the original ship schedule at voyage leg p (knots)
$\delta_p^{port} \in \mathbb{R}^+ \forall p \in P$	anticipated duration of port p disruption (hours)
$\delta_p^{sea} \in \mathbb{R} \forall p \in P$	anticipated ship speed change at disrupted voyage leg p (knots)
$y_p^{port} \in \mathbb{B} \forall p \in P$	=1 if port p is disrupted (else = 0)
$y_p^{sea} \in \mathbb{B} \forall p \in P$	=1 if voyage leg p is disrupted (else = 0)
$z_p^{skip} \in \mathbb{B} \forall p \in P$	=1 if skipping disrupted port p is feasible (else = 0)
$y_{pp^*} \in \mathbb{B} \forall p, p^* \in P, p \neq p^*$	=1 if diverting the cargo from disrupted port p to port p^* is feasible (else = 0)
$C_p^{port} \in \mathbb{R}^+ \forall p \in P$	available capacity of the port terminal to accommodate the diverted containers at port p (TEUs)
$C_p^{land} \in \mathbb{R}^+ \forall p \in P$	available capacity for inland transportation of the diverted containers at port p (TEUs)
$c_{ph}^{port} \in \mathbb{R}^+ \forall p \in P, h \in H_p$	unit cost related to container handling at port p with handling rate h (USD/TEU)
$c_p^{fuel} \in \mathbb{R}^+ \forall p \in P$	unit fuel consumption cost at voyage leg p (USD/ton)
$c^{oper} \in \mathbb{R}^+$	unit basic ship operational cost (USD/hour)
$c_p^{skip} \in \mathbb{R}^+ \forall p \in P$	cost related to skipping port p (USD)
$c_p^{mis} \in \mathbb{R}^+ \forall p \in P$	unit misconnected cargo cost at port p (USD/TEU)
$c_{pp^*}^{d-port} \in \mathbb{R}^+ \forall p, p^* \in P, p \neq p^*$	unit cost related to handling diverted containers from disrupted port p to port p^* (USD/TEU)
$c_{pp^*}^{d-land} \in \mathbb{R}^+ \forall p, p^* \in P, p \neq p^*$	unit cost related to inland transportation of containers diverted from disrupted port p to port p^* (USD/TEU)

(continued on next page)

(*continued*)

Parameters	Description of Parameters
$c_p^{cargo} \in \mathbb{R}^+ \forall p \in P$	unit freight rate that a shipping line can accumulate after cargo delivery at port p (USD/TEU)
$SOC \in \mathbb{R}^+$	total original cost related to basic ship operations (USD)
$TP \in \mathbb{R}^+$	total original profit anticipated by the shipping line (USD)

4.2. Mathematical model

A mixed-integer non-linear programming model for the Multi-Objective Ship Schedule Recovery Problem, abbreviated as **MOSSR-1**, can be formulated using the following objective functions and constraint sets. The first objective function (F_1) of **MOSSR-1**, represented by equation (4.1), aims to minimize the total late ship arrivals at ports. The second objective function (F_2) of **MOSSR-1**, represented by equation (4.2), seeks to minimize the total profit loss, and its constituent parts are motivated by economic considerations that include the following: (i) total original profit; (ii) total recovered revenue; (iii) operational cost of the ships; (iv) total recovered bunker fuel consumption cost; (v) total recovered container handling cost; and (vi) total cost of container diversion.

$$minF_1 = \sum_{p \in P} \overline{\tau_p^{del}} \tag{4.1}$$

$$minF_2 = TP - (\overline{REV} - SOC - \overline{FCC} - \overline{TPC} - \overline{CDC}) \tag{4.2}$$

The constraint sets of **MOSSR-1** can be divided into six groups. Constraints (4.3) through (4.7) form the first constraint group of the **MOSSR-1** model devoted to sailing speed and bunker fuel consumption estimations. Constraint set (4.3) computes the recovered ship sailing speed at every voyage leg, considering the possible sea disruptions and ship sailing speed adjustments. In particular, the recovered ship sailing speed at voyage leg p ($\overline{s_p}, p \in P$) is estimated based on the planned ship sailing speed at that voyage leg ($s_p, p \in P$), anticipated change in ship sailing speed due to a disruption ($\delta_p^{sea}, p \in P$), and sailing speed adjustment of a ship at that voyage leg ($\Delta_p^{sea}, p \in P$). Note that the ship sailing speed adjustment decision variable is multiplied by the term "$(1 - y_p^{sea})$", where $y_p^{sea} = 1$ if voyage leg p experiences a disruption (else $= 0$). Therefore, the ship sailing speed adjustment cannot be implemented at voyage legs that are subject to disruptions. Such an assumption can be justified by the fact that it may be difficult or even impossible for a ship to maintain a specific speed level and/or reach the desired speed adjustment level at the disrupted voyage legs due to added resistance, unfavorable winds, waives, currents, etc. (Du et al., 2021; Du et al., 2022b). The upper and lower bounds of ship recovered sailing speed are defined by constraint sets (4.4) and (4.5), respectively. On the other hand, constraint sets (4.6) and (4.7) compute the recovered ship sailing time and recovered bunker fuel consumption of ships at every voyage leg, respectively.

$$\overline{s_p} = s_p + \delta_p^{sea} \bullet y_p^{sea} + \Delta_p^{sea} \bullet (1 - y_p^{sea}) \forall p \in P \tag{4.3}$$

$$\overline{s_p} \leq s^{max} \forall p \in P \tag{4.4}$$

$$\overline{s_p} \geq s^{min} + \delta_p^{sea} \bullet y_p^{sea} \forall p \in P \tag{4.5}$$

$$\overline{\tau_p^{sail}} = \frac{d_p^{leg}}{\overline{s_p}} \forall p \in P \tag{4.6}$$

$$\overline{f_p} = \frac{\gamma(\overline{s_p})^{(\alpha-1)}}{24} \bullet \left(\frac{d_p^{sea} \bullet AWT + LWT}{TWT + LWT} \right)^{2/3} \forall p \in P \tag{4.7}$$

Constraint sets (4.8) through (4.14) form the second constraint group of the **MOSSR-1** model, which estimates the major recovered time elements related to ship service at ports. These time components are as follows: (1) recovered ship waiting time at ports (computed using constraints (4.8) and (4.9)); (2) recovered ship arrival time at ports (computed using constraints (4.10) and (4.11)); (3) recovered ship arrival delays (computed using constraints (4.12)); (4) recovered ship departure time from ports (computed using constraints (4.13)); and (5) recovered total ship turnaround time (computed using constraints (4.14)).

$$\overline{\tau_{(p+1)}^{wait}} \geq \tau_{(p+1)}^{st} - (\overline{\tau_p^{dep}} + \overline{\tau_p^{sail}}) \forall p \in P, p < n \tag{4.8}$$

$$\overline{\tau_{(1)}^{wait}} \geq \tau_{(1)}^{st} - (\overline{\tau_p^{dep}} + \overline{\tau_p^{sail}}) + \overline{STT} \forall p \in P, p = n \tag{4.9}$$

$$\overline{\tau_{(p+1)}^{arr}} = \overline{\tau_p^{dep}} + \overline{\tau_p^{sail}} \forall p \in P, p < n \tag{4.10}$$

$$\overline{\tau_{(1)}^{arr}} = \overline{\tau_p^{dep}} + \overline{\tau_p^{sail}} - \overline{STT} \forall p \in P, p = n \tag{4.11}$$

$$\overline{\tau_p^{del}} \geq \overline{\tau_p^{arr}} - \tau_p^{arr} \forall p \in P \tag{4.12}$$

$$\overline{\tau_p^{dep}} = \overline{\tau_p^{arr}} + \overline{\tau_p^{wait}} + \overline{\tau_p^{hand}} \forall p \in P \tag{4.13}$$

$$\overline{STT} = \sum_{p \in P} \overline{\tau_p^{sail}} + \sum_{p \in P} \overline{\tau_p^{wait}} + \sum_{p \in P} \overline{\tau_p^{hand}} \tag{4.14}$$

Constraint sets (4.15) through (4.19) form the third constraint group of the **MOSSR-1** model, aiming to determine the feasibility of container diversion option and the ports that will handle the diverted demand. Constraint set (4.15) ensures that only disrupted ports could be skipped by the shipping line. Constraint set (4.16) assures that a port can only be skipped if it is a viable option. Constraint set (4.17) specifies that the container demand can be diverted from a port only if the port is skipped. Constraint set (4.18) ensures that the diversion of containers from a skipped port to alternative ports is possible. Constraint set (4.19) specifies which ports will receive the diverted containers from the disrupted ports.

$$x_p^{skip} \leq y_p^{port} \forall p \in P \tag{4.15}$$

$$x_p^{skip} \leq z_p^{skip} \forall p \in P \tag{4.16}$$

$$x_{pp^*}^{div} \leq x_p^{skip} \forall p, p^* \in P, p \neq p^* \tag{4.17}$$

$$x_{pp^*}^{div} \leq y_{pp^*} \forall p, p^* \in P, p \neq p^* \tag{4.18}$$

$$x_{p^*}^{dd} \leq \sum_{p \in P: p \neq p^*} x_{pp^*}^{div} \forall p^* \in P \tag{4.19}$$

Constraint sets (4.20) through (4.26) form the fourth constraint group of the **MOSSR-1** model, aiming to ensure the feasibility of handling the diverted containers at alternative ports and compute the recovered ship handling time. The diverted container demand to an alternative port is calculated by constraint set (4.20). Constraint set (4.21) ensures that the container demand to be diverted from a given port will not exceed the original container demand of that port. Constraint set (4.22) assures that the existing capacity at the selected alternative port is adequate to meet the diverted demand. Constraint set (4.23) ensures that the inland transportation capacity of the selected alternative port is sufficient to distribute the diverted container demand to the respective destinations. Constraint set (4.24) calculates the recovered number of containers to be handled at each port. Constraint set (4.25) guarantees that only one of the available container handling rates will be selected at each port. Constraint set (4.26) computes the recovered container handling time while considering the possibility of skipping a disrupted port and cargo diversion.

$$d_{pp^*}^{div} = d_p^{port} \bullet x_{pp^*}^{div} \forall p, p^* \in P, p \neq p^* \tag{4.20}$$

$$\sum_{p^* \in P: p^* \neq p} d_{pp^*}^{div} \leq d_p^{port} \forall p \in P \tag{4.21}$$

$$\sum_{p \in P: p \neq p^*} d_{pp^*}^{div} \leq C_{p^*}^{port} \bullet x_{p^*}^{dd} \forall p^* \in P \tag{4.22}$$

$$\sum_{p \in P: p \neq p^*} d_{pp^*}^{div} \leq C_{p^*}^{land} \bullet x_{p^*}^{dd} \forall p^* \in P \tag{4.23}$$

$$\overline{d_{p^*}^{port}} = d_{p^*}^{port} \bullet \left(1 - x_{p^*}^{skip}\right) + \sum_{p \in P: p \neq p^*} d_{pp^*}^{div} \forall p^* \in P \tag{4.24}$$

$$\sum_{h \in H_p} \overline{x_{ph}} = 1 \forall p \in P \tag{4.25}$$

$$\overline{\tau_p^{hand}} = [\sum_{h \in H_p} \left(\frac{\overline{d_p^{port}}}{pr_{ph}}\right) \bullet \overline{x_{ph}} + \delta_p^{port} \bullet y_p^{port}] \bullet \left(1 - x_p^{skip}\right) \forall p \in P \tag{4.26}$$

Constraint sets (4.27) through (4.29) form the fifth constraint group of the **MOSSR-1** model, which ensures that the changes in the number of containers on board the ships will stay within the acceptable limits defined by the capacity of deployed ships. In particular, constraint sets (4.27) and (4.28) compute the total number of containers to be transported by the ship at each voyage leg for the recovered ship schedule, taking into account port skipping and container diversion decisions. Constraint set (4.29) assures that the total number of containers on board each ship will not exceed its capacity.

$$\begin{aligned} d_{(p^*+1)}^{sea} = d_{p^*}^{sea} - \left[d_{(p^*+1)}^{port} \bullet IMP_{(p^*+1)} - d_{(p^*+1)}^{port} \bullet \left(1 - IMP_{(p^*+1)}\right)\right] \\ \bullet (1 - x_{(p^*+1)}^{skip}) - \sum_{p \in P: p \neq (p^*+1)} d_{p(p^*+1)}^{div} \bullet IMP_p + \sum_{p \in P: p \neq (p^*+1)} d_{p(p^*+1)}^{div} \\ \bullet \left(1 - IMP_p\right) \forall p^* \in P, p^* < n \end{aligned} \tag{4.27}$$

$$\begin{aligned} d_{(1)}^{sea} = d^{sea-0} - \left[d_{(1)}^{port} \bullet IMP_{(1)} - d_{(1)}^{port} \bullet \left(1 - IMP_{(1)}\right)\right] \\ \bullet (1 - x_{(1)}^{skip}) - \sum_{p \in P: p \neq (1)} d_{p(1)}^{div} \bullet IMP_p + \sum_{p \in P: p \neq (1)} d_{p(1)}^{div} \bullet \left(1 - IMP_p\right) \end{aligned} \tag{4.28}$$

$$d_p^{sea} \bullet AWT \leq TWT \forall p \in P \tag{4.29}$$

Constraints (4.30) through (4.34) form the sixth and final constraint group of the **MOSSR-1** model, which estimates all of the individual cost elements required for the calculation of the **MOSSR-1** objective functions (4.1) and (4.2). In particular, the total operational cost is calculated using constraint set (4.30). Constraint sets (4.31)-(4.34) compute the recovered total fuel cost, recovered total port handling cost, recovered total container diversion cost, and recovered total revenue.

$$SOC = c^{oper} \bullet \varphi \bullet V \tag{4.30}$$

$$\overline{FCC} = \sum_{p \in P} c_p^{fuel} \bullet d_p^{leg} \bullet \overline{f_p} \tag{4.31}$$

$$\overline{TPC} = \sum_{p \in P} \sum_{h \in H_p} c_{ph}^{port} \bullet d_p^{port} \bullet \overline{x_{ph}} + \sum_{p \in P} (c_p^{skip} + c_p^{mis} \bullet d_p^{port}) \bullet x_p^{skip} \tag{4.32}$$

$$\overline{CDC} = \sum_{p \in P} \sum_{p^* \in P} (c_{pp^*}^{d-port} + c_{pp^*}^{d-land}) \bullet d_{pp^*}^{div} \tag{4.33}$$

$$\overline{REV} = \sum_{p \in P} c_p^{cargo} \bullet d_p^{port} \bullet \left(1 - x_p^{skip}\right) + \sum_{p \in P} \sum_{p^* \in P} c_p^{cargo} \bullet d_{pp^*}^{div} \tag{4.34}$$

5. Proposed solution approach

This section contains a detailed description of the solution methodology proposed, including the **MOSSR-1** mathematical model linearization procedures and an exact multi-objective optimization algorithm for ship scheduling recovery.

5.1. Preliminary linearization procedures

Constraint sets (4.6), (4.7), and (4.26) are normally used in liner shipping studies to estimate recovered ship sailing time, recovered bunker fuel consumption, and recovered port handling time, respectively (Wang et al., 2014; Abioye et al., 2019; Abioye et al., 2021). However, these constraint sets make the **MOSSR-1** mathematical model non-linear. The **MOSSR-1** model can be reduced in computational complexity using certain linearization procedures. First, the recovered and original ship sailing speeds can be replaced with their reciprocals ($v_p = \frac{1}{s_p} \forall p \in P$; $\dot{v}_p = \frac{1}{\dot{s}_p} \forall p \in P$). Accordingly, the projected sailing speed decrease due to disruptive incidents ($\delta_p^{sea}, p \in P$ – knots) and the adjustment in ship sailing speed ($\Delta_p^{sea}, p \in P$ – knots) will have to be modified as well. Let $\dot{\delta}_p^{sea}, p \in P$ (knots^{-1}) and $\dot{\Delta}_p^{sea}, p \in P$ (knots^{-1}) specify the projected ship sailing speed decrease and the adjustment in ship sailing speed at voyage leg p, respectively. Second, the non-linear bunker fuel consumption function for the recovered ship schedule $\overline{f_p}, p \in P$ (tons) can be linearized using the piecewise linear secant approximation method, which has been widely used in the liner shipping literature (Wang and Meng, 2012a; Wang et al., 2013). Hence, the recovered linear bunker fuel consumption function $\overline{FC_{pk}}, p \in P, k \in K$ can be represented with a set of secant segments denoted as $K = \{1, \cdots, k\}$.

For the purpose of linear bunker fuel consumption function modeling, additional variable $b_{pk}, p \in P, k \in K$ can be introduced, such that $b_{pk} = 1$ if the bunker fuel consumption at voyage leg p is estimated using linear secant segment k (else = 0). Let $st_k, ed_k, k \in K$ denote the reciprocal ship speed values at the start and at the end of linear secant segment k; $SL_k, IN_k, k \in K$ specify the values for the slope and the intercept of linear secant segment k; and M_1 and M_2 represent comparatively big positive numbers. Then, the **MOSSR-2** mathematical model, which is a partial linearization of the **MOSSR-1** model, can be formulated using objective functions (5.1) and (5.2) and constraint sets (4.8)-(4.30), (4.32)-(4.34), and (5.3)-(5.11) as follows:

Partially Linearized Multi-Objective Ship Schedule Recovery Problem (**MOSSR-2**):

$$minF_1 = \sum_{p \in P} \overline{\tau_p^{del}} \tag{5.1}$$

$$minF_2 = TP - (\overline{REV} - SOC - \overline{FCC} - \overline{TPC} - \overline{CDC}) \tag{5.2}$$

Subject to: Constraint sets (4.8)-(4.30) and (4.32)-(4.34)

$$v_p = \dot{v}_p + \dot{\delta}_p^{sea} \bullet y_p^{sea} + \dot{\Delta}_p^{sea} \bullet (1 - y_p^{sea}) \forall p \in P \tag{5.3}$$

$$v_p \geq \frac{1}{s^{max}} \forall p \in P \tag{5.4}$$

$$v_p \leq \frac{1}{s^{min}} + \dot{\delta}_p^{sea} \bullet y_p^{sea} \forall p \in P \tag{5.5}$$

$$\overline{\tau_p^{sail}} = d_p^{leg} \bullet v_p \forall p \in P \tag{5.6}$$

$$\sum_{k \in K} b_{pk} = 1 \forall p \in P \tag{5.7}$$

$$st_k \bullet b_{pk} \leq v_p \forall p \in P, k \in K \tag{5.8}$$

$$ed_k + M_1 \bullet \left(1 - b_{pk}\right) \geq v_p \forall p \in P, k \in K \tag{5.9}$$

$$\overline{FC_{pk}} \geq (SL_k \bullet v_p + IN_k) \bullet \left(\frac{d_p^{sea} \bullet AWT + LWT}{TWT + LWT}\right)^{2/3} - M_2 \bullet (1 - b_{pk}) \forall p \in P, k \in K \tag{5.10}$$

$$\overline{FCC} = \sum_{p \in P} \sum_{k \in K} c_p^{fuel} \bullet d_p^{leg} \bullet \overline{FC}_{pk} \tag{5.11}$$

The first objective function (5.1) in the proposed **MOSSR-2** mathematical model aims to minimize the total late ship arrivals at ports, while the second objective function (5.2) aims to minimize the total profit loss. The reciprocal value of sailing speed is calculated using constraint set (5.3) at every voyage leg for the recovered schedule. The reciprocal value limits for sailing speed are defined using constraint sets (5.4) and (5.5). Constraint set (5.6) uses the reciprocal value of sailing speed to compute ship sailing time for the recovered schedule at every voyage leg. Constraint set (5.7) assures that just one linear segment is used to calculate the recovered bunker fuel consumption of ships at every voyage leg. Constraint sets (5.8) and (5.9) define the maximum and minimum reciprocal values of sailing speed that can be adopted to compute the recovered bunker fuel consumption of ships at a given voyage leg using the selected linear segment. The recovered bunker fuel consumption of ships is computed by constraint set (5.10) using the reciprocal value of sailing speed at every voyage leg. The total recovered fuel cost to be imposed to the shipping line is determined by constraint set (5.11).

Fig. 4 shows linearized approximations of non-linear bunker fuel consumption function with one, two, three, and four linear secant segments. Based on the previous studies related to liner shipping operations, the upper and lower bounds for the ship's sailing speed were limited to 15 and 25 knots (Pasha et al., 2021), while the value of bunker fuel consumption was obtained using the following function: $FC(v) = \frac{0.012 \bullet (v)^{-2}}{24}$. The provided examples clearly show that the level of accuracy for the fuel consumption approximating function improves as the number of linear secant segments increases. Nevertheless, the linearization procedures adopted herein are unable to fully linearize the entire optimization model due to the presence of a highly non-linear constraint set (4.26), which estimates the recovered port handling time.

5.2. Exact multi-objective optimization algorithm

In contrast to single-objective optimization models, multi-objective optimization models do not have just one solution that contains the best values for all the considered objective functions. In particular, the **MOSSR-2** mathematical formulation has two conflicting objective functions, and the best possible value of one objective function will lead to the worst value for the second objective function. As mentioned earlier, a variety of recovery options could be implemented by the shipping line to reduce or completely eliminate the delays (i.e., minimize the value of F_1) due to the occurrence of disruptive incidents, including port skipping without the diversion of containers to alternative ports, port skipping with the diversion of containers to alternative ports, increasing ship sailing speeds at specific voyage legs, and increasing ship handling rates at specific ports. However, the shipping line will incur additional costs in order to implement any of the aforementioned recovery options (i.e., an increase in the value of F_2 will be observed). On the contrary, taking measures to reduce the total cost, such as decreasing the sailing speed to reduce the total fuel consumption cost (improving F_2), may increase the total delay (worsening F_1). Within the context of multi-objective optimization, a Pareto Front (PF) is a collection of optimal solutions that are not dominated by other solutions. This set of solutions does not allow for any of the objective functions to be improved upon without negatively impacting the performance of the other functions (Dulebenets, 2018; Mavrotas, 2009). For multi-objective optimization, PFs can be used to analyze tradeoffs between competing objectives and find the best solution that compromises these objectives.

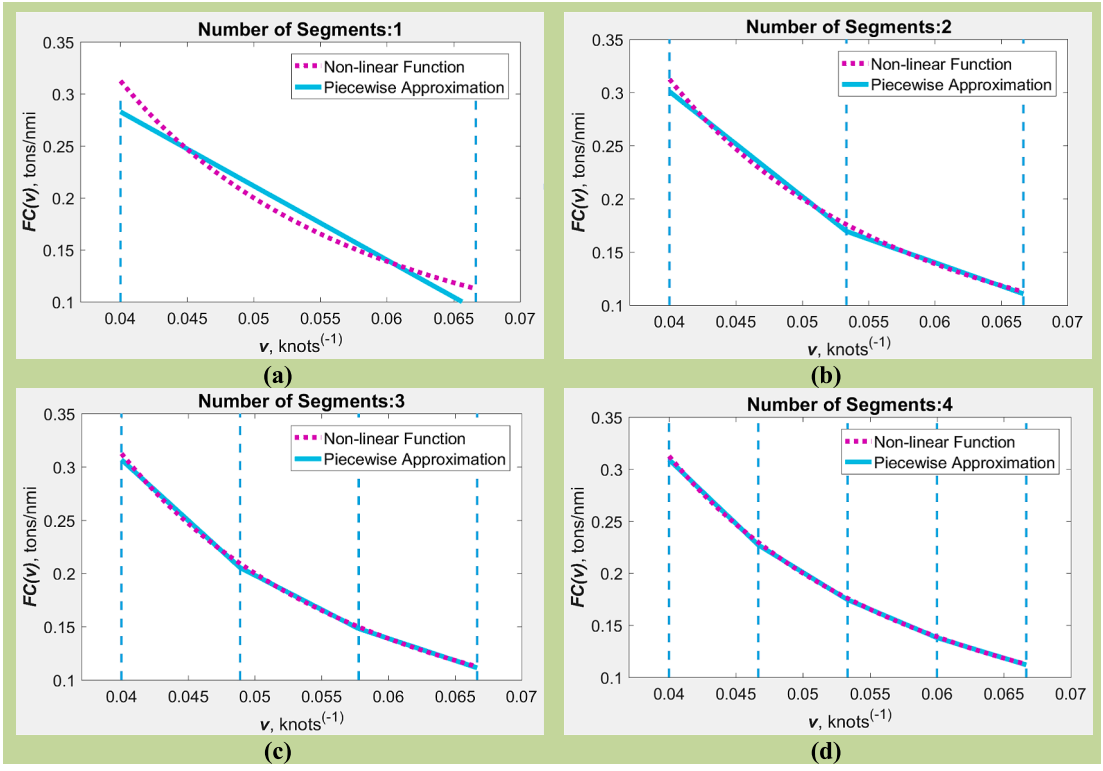

Fig. 4. Examples of recovered bunker fuel consumption approximations with: (a) one linear secant segment; (b) two linear secant segments; (c) three linear secant segments; and (d) four linear secant segments.

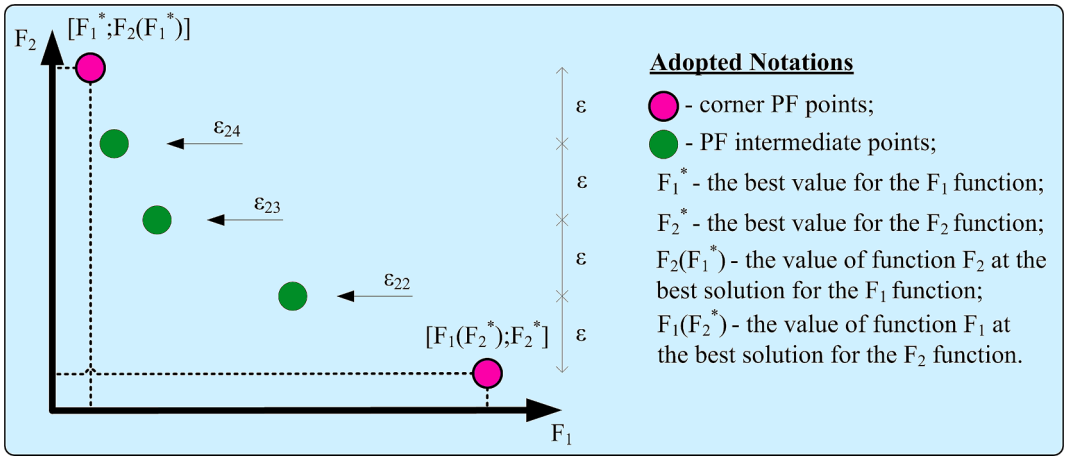

Fig. 5. Illustration of the corner and intermediate PF points.

An Exact Multi-Objective Optimization Algorithm for Ship Schedule Recovery (EMOA-SSR) was adopted in this study to develop PFs for the **MOSSR-2** mathematical model. The EMOA-SSR algorithm is inspired by the epsilon-constraint method, which is one of the most popular exact algorithms for multi-objective optimization (Mavrotas, 2009). In the epsilon-constraint method, the most important practical objective function is minimized, while the other objective function is limited by an upper bound. Then, by repeatedly modifying the upper bound values, the Pareto Front (PF) is generated. Pseudocode 1 (**PS-1**) outlines the primary EMOA-SSR steps. First, a data structure is created to store the PF points. Then, the corner PF points are determined in steps 2 and 3. The corner PF point $[F_1^*;F_2(F_1^*)]$ represents a solution that has the minimum F_1 value, and the F_2 is constrained by an upper bound ε_2. Likewise, the corner PF point $[F_1(F_2^*);F_2^*]$ represents a solution that has the minimum F_2 value, and the F_1 is constrained by an upper bound ε_1. The corner PF points $[F_1^*;F_2(F_1^*)]$ and $[F_1(F_2^*);F_2^*]$ will be obtained by solving the **MOSSR-2-F1** and **MOSSR-2-F2** mathematical models, which can be formulated as follows:

Partially Linearized Multi-Objective Ship Schedule Recovery Problem with the F_1 minimization (**MOSSR-2-F1**):

$$minF_1 = \sum_{p\in P}\overline{\tau_p^{del}} \tag{5.12}$$

Subject to: (4.8)-(4.30), (4.32)-(4.34), and (5.3)-(5.11)

$$F_2 = TP - (\overline{REV} - SOC - \overline{FCC} - \overline{TPC} - \overline{CDC}) \tag{5.13}$$

$$F_2 \le \varepsilon_2 \tag{5.14}$$

Partially Linearized Multi-Objective Ship Schedule Recovery Problem with the F_2 minimization (**MOSSR-2-F2**):

$$minF_2 = TP - (\overline{REV} - SOC - \overline{FCC} - \overline{TPC} - \overline{CDC}) \tag{5.15}$$

Subject to: (4.8)-(4.30), (4.32)-(4.34), and (5.3)-(5.11)

$$F_1 = \sum_{p\in P}\overline{\tau_p^{del}} \tag{5.16}$$

$$F_1 \le \varepsilon_1 \tag{5.17}$$

PS-1. Exact Multi-Objective Optimization Algorithm for Ship Schedule Recovery (EMOA-SSR)

EMOA-SSR$(InputData, N_{PF}, \varepsilon_1, \varepsilon_2)$

in: *InputData* - input parameters for **MOSSR-2**; N_{PF} - total defined number of PF points; ε_1 - upper bound on the objective F_1; ε_2 - upper bound on the objective F_2

out: *PF* - PF set identified for **MOSSR-2**

(*continued on next column*)

(*continued*)

1: $|PF| \leftarrow N_{PF}$ ◁ Establishment of the PF storing data structure
2: $[F_1^*;F_2(F_1^*)] \leftarrow$ ***MOSSR-2-F1***$(InputData, \varepsilon_2)$ ◁ Identify the corner point F_1^*
3: $[F_1(F_2^*);F_2^*] \leftarrow$ ***MOSSR-2-F2***$(InputData, \varepsilon_1)$ ◁ Identify the corner point F_2^*
4: $\varepsilon \leftarrow \frac{F_2(F_1^*) - F_2^*}{(N_{PF}-1)}$ ◁ Determine the upper bound interval for F_2
5: $i \leftarrow 1$ ◁ Start the iteration counter
6: $\varepsilon_{2i} \leftarrow F_2^*$ ◁ Establish the first F_2 upper bound
7: $PF \leftarrow PF \cup [F_1(F_2^*);F_2^*]$ ◁ Add the corner point F_2^*
8: **while** $|PF| \le (N_{PF}-2)$ **do**
9: $i \leftarrow i+1$ ◁ Update the iteration counter
10: $\varepsilon_{2i} \leftarrow \varepsilon_{2i} + \varepsilon$ ◁ Update the ε_{2i} value
11: $[F_{1i}^*;F_2(F_{1i}^*)] \leftarrow$ ***MOSSR-2-F1***$(InputData, \varepsilon_{2i})$ ◁ Solve ***MOSSR-2-F1*** with the updated ε_{2i}
12: $PF \leftarrow PF \cup [F_{1i}^*;F_2(F_{1i}^*)]$ ◁ Add the PF point generated in the previous step
13: **end while**
14: $PF \leftarrow PF \cup [F_1^*;F_2(F_1^*)]$ ◁ Add the corner point $[F_1^*;F_2(F_1^*)]$
15: **return** *PF*

The illustration of corner PF points $[F_1^*;F_2(F_1^*)]$ and $[F_1(F_2^*);F_2^*]$ is provided in Fig. 5. The objective F_2 values at the two corner PF points along with the total number of PF points (N_{PF}) are used in step 4 in the equation that determines the upper bound interval for F_2 (this interval is denoted as ε). In step 6, the initial F_2 upper bound (ε_{2i}) is set to F_2^*. Next, in step 7, the construction of the PF begins with the point F_2^*; more specifically, the corner PF point $[F_1(F_2^*);F_2^*]$ is added to the PF data structure. Then, in steps 8–13, the EMOA-SSR algorithm begins an iterative procedure. Within the loop in step 10, the value for the F_2 upper bound increases by ε at each iteration. In step 11, the **MOSSR-2-F1** mathematical model is solved using the established upper bound on F_2, and a new PF point is produced. Step 12 adds the newly generated point to the PF data structure. The process terminates when the number of newly generated PF points reaches $N_{PF}-1$. After the required algorithmic iterations have been completed, the EMOA-SSR algorithm will move on to step 14 and append the final PF point. This point will correspond to the best possible solution for the objective F_1 ($[F_1^*;F_2(F_1^*)]$).

6. Computational experiments

The following sections of the manuscript present the results of numerical experiments designed to assess the computational performance of the adopted EMOA-SSR algorithm and demonstrate the ability of the presented multi-objective mathematical formulation to provide useful managerial insights. A set of analyses were performed on a Dell system equipped with an Intel(R) CoreTMi7 processor and 32 GB of RAM. The EMOA-SSR algorithm was implemented in MATLAB 2021b. The EMOA-

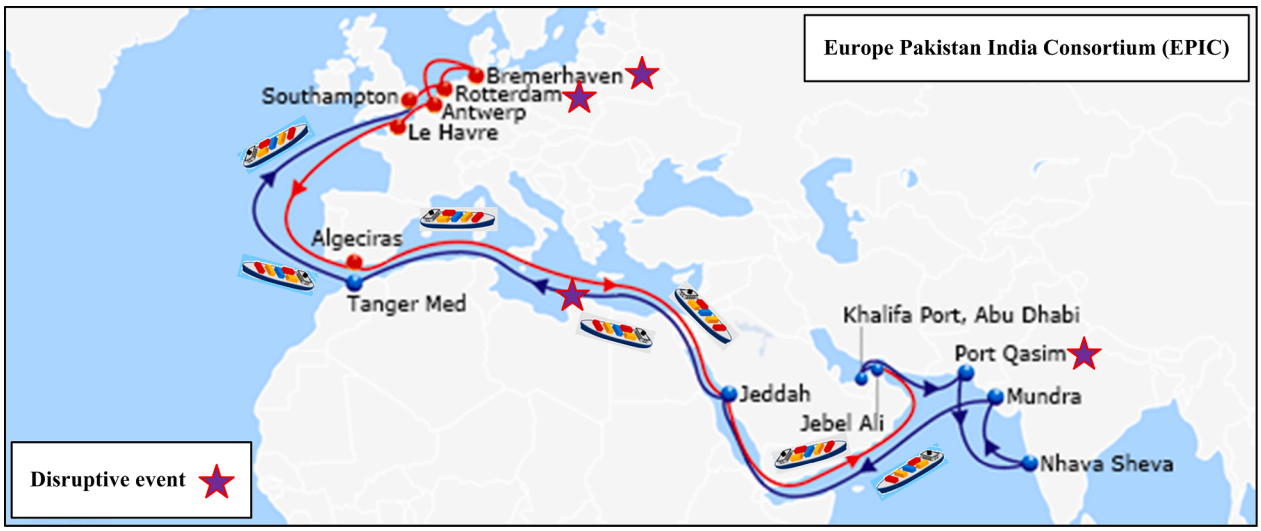

Fig. 6. Illustration of the Europe Pakistan India Consortium shipping route.

SSR algorithm directly relies on the **MOSSR-2-F1** and **MOSSR-2-F2** mathematical models, which were both coded using the GAMS software and solved using BARON with the target optimality gap of 0.1%.

6.1. Input data adopted

The numerical experiments were carried out for the EPIC (Europe Pakistan India Consortium) shipping route. Currently, the Compagnie Maritime d'Affrètement and Compagnie Générale Maritime (generally referred to as "CMA CGM") serves this shipping route (CMA CGM, 2022). The considered transit route with a total of 14 ports of call provides a maritime connection between North Europe, Middle East, and India. The Port of Jeddah (Saudi Arabia) is visited twice by the ships deployed under normal operational conditions. Fig. 6 depicts a graphical representation of the considered shipping route. The list of port visits and distances between these ports (shown in square brackets and expressed in nautical miles) can be presented as follows (Ports.com, 2022):

1. Port of Jebel Ali, United Arab Emirates [302] → 2. Port of Khalifa, United Arab Emirates [748] → 3. Port Qasim, Pakistan [1,113] → 4. Port of Nhava Sheva, India [429] → 5. Port of Mundra, India [2,496] → 6. Port of Jeddah, Saudi Arabia [3,035] → 7. Tanger Med Port, Morocco [1,367] → 8. Port of Southampton, England [293] → 9. Port of Rotterdam, Netherlands [309] → 10. Port of Bremerhaven, Germany [393] → 11. Port of Antwerp, Belgium [244] → 12. Port of Le Havre, France [1,397] → 13. Port of Algeciras, Spain [3,006] → 14. Port of Jeddah, Saudi Arabia [2,371] → 1. Port of Jebel Ali, United Arab Emirates.

Table 2 shows the input data that were adopted for the mixed integer multi-objective ship schedule recovery mathematical model throughout the conducted computational experiments. The numerical data were derived primarily from the existing literature on liner shipping (Wang and Meng, 2012a,b; Wang et al., 2014; Alharbi et al., 2015; Pasha et al., 2020; Abioye et al., 2021; CMA CGM, 2022; PBT International, 2022). Note that since the EPIC shipping route is passing through the emission control areas (i.e., English Channel and North Sea), it was assumed that the shipping line had to use ultra-low sulfur fuel oil (ULSFO) within the emission control areas and very-low sulfur fuel oil (VLSFO) outside the emission control areas.

In order to obtain useful managerial insights for shipping lines using the developed multi-objective mathematical model, five possible disruption scenarios were considered. In the **first scenario**, it was assumed that the disruptive incidents occurred at sea and ports. In particular, the Port of Qasim (Pakistan), the Port of Rotterdam (Netherlands), and the Port of Bremerhaven (Germany) all experienced

Table 2
The values of the parameters used in computational experiments.

Parameter	Value
Number of ports to be visited: n (port visits)	14
Number of offered handling rates at ports: m (port handling rates)	3
Demand for containers at ports: $d_p^{port}, p \in P$ (TEUs)	$U[200; 2,000]$
Percentage of import containers at ports: $IMP_p, p \in P$ (%)	$U[40; 60]$
Container handling productivity: $pr_{ph}, p \in P, h \in H_p$ (TEUs/hour)	$U[50; 200]$
Negotiated service frequency of ports: φ (hours)	168
Number of allocated ships: V (ships)	10
Coefficients of fuel consumption: α, γ	$\alpha = 3.0, \gamma = 0.012$
Standardized 20-foot container cargo weight: AWT (tons)	9
Total ship empty weight: LWT (tons)	50,000
Total ship maximum allowable container weight: TWT (tons)	200,000
Payload of the ship prior to docking at its first port: d^{sea-0} (TEUs)	$U[4,000; 7,000]$
Minimum allowed speed for ships: s^{min} (knots)	15
Maximum allowed speed for ships: s^{max} (knots)	25
Original sailing speed of ships: $s_p, p \in P$ (knots)	$U[15; 18]$
Duration anticipated for disruptive incidents at ports: δ_p^{port}, $p \in P$ (hours)	$U[10; 100]$
Variation anticipated in the ship speed due to disruptive incidents: $\delta_p^{sea}, p \in P$ (knots)	$-U[1.0; 3.0]$
Handling capacity at ports to meet the diverted demand: $C_p^{port}, p \in P$ (TEUs)	$U[200; 2,000]$
Capacity for inland transportation to meet the diverted demand: $C_p^{land}, p \in P$ (TEUs)	$U[200; 2,000]$
Unit cost of ship handling at ports: $c_{ph}^{port}, p \in P, h \in H_p$ (USD/TEU)	$hc^{av} \pm U[0; 50]$
Average cost of ship handling at ports: hc^{av} (USD/TEU)	$U[400; 700]$
Unit fuel consumption cost: $c_p^{fuel}, p \in P$ (USD/ton)	800 (VLSFO); 1,200 (ULSFO)
Unit basic ship operational cost: c^{oper} (USD/hour)	(350,000/168)
Cost of port skipping: $c_p^{skip}, p \in P$ (USD)	$\mu \cdot hc^{av} \cdot d_p^{port}$
Inconvenient factor of port skipping: μ	1.10
Unit penalty for misconnected containers at ports: $c_p^{mis}, p \in P$ (USD/TEU)	$U[50; 100]$
Unit cost of handling diverted containers: $c_{pp^*}^{d-port}, p, p^* \in P, p \neq p^*$ (USD/TEU)	$U[400; 700]$
Unit cost of inland transportation of containers: $c_{pp^*}^{d-land}, p, p^* \in P, p \neq p^*$ (USD/TEU)	$U[600; 800]$
Unit cost of container shipping between ports p and $p+1$: $c_p^{cargo}, p \in P$ (USD/TEU)	$U[4,000; 6,000]$
Total original profit anticipated by the shipping line: TP (USD)	70,000,000

disruptions in port operations due to severe weather. The disruptions were expected to last for $\delta_3^{port} = 79$ hours, $\delta_9^{port} = 78$ hours, and $\delta_{10}^{port} = 49$ hours, respectively. In addition, a pirate attack at voyage leg "6" between the Port of Jeddah (Saudi Arabia) and the Port of Tanger Med (Morocco) caused a sailing speed reduction of $\delta_6^{sea} = 1.34$ knots. The first disruption scenario was assumed to be the base scenario. In the **second scenario**, the disruptive incidents occurred at ports of call only. More specifically, the Port of Qasim (Pakistan), the Port of Rotterdam (Netherlands), and the Port of Bremerhaven (Germany) all experienced disruptions with the expected duration of $\delta_3^{port} = 79$ hours, $\delta_9^{port} = 78$ hours, and $\delta_{10}^{port} = 49$ hours, respectively.

In the **third scenario**, the disruptive incidents were assumed to happen at the port early in the ship voyage. In particular, the Port of Qasim (Pakistan) experienced a disruptive incident with the expected duration of $\delta_3^{port} = 79$ hours. In the **fourth scenario**, the disruptive incidents occurred at the ports later in the ship voyage. More specifically, ship services were disrupted at the Port of Rotterdam (Netherlands) and the Port of Bremerhaven (Germany). The disruptive incidents were projected to last for $\delta_9^{port} = 78$ hours and $\delta_{10}^{port} = 49$ hours, respectively. In the **fifth scenario**, no disruptive incidents were reported during the ship voyage. This is a perfect scenario in which the original schedule of the liner shipping company is not interrupted at any point during the voyage.

6.2. Solution methodology assessment

Time complexity is a crucial metric to consider when assessing the computational performance of the adopted solution approach. Algorithms requiring excessive processing time to produce solutions are undesirable. As previously stated, the adopted EMOA-SSR algorithm is inspired by the canonical ECON method. Therefore, the EMOA-SSR time complexity will be affected with the PF size – $|PF|$. Furthermore, the EMOA-SSR time complexity will be influenced with the number of linear secant segments used in the approximation for the bunker fuel consumption function – $|K|$ (see Fig. 4). An increase in the number of linear secant segments in the approximating function would increase the size of the **MOSSR-2-F1** and **MOSSR-2-F2** mathematical models and, hence, will increase the EMOA-SSR computational time. In order to perform the time complexity analysis of the EMOA-SSR algorithm, a total of 81 scenarios were developed. The desired number of PF points increased from four to twenty (with a two-point increment), and the number of linear secant segments increased from four to twelve (with a one-point increment). The analysis was conducted for the base disruption scenario with disruptive incidents at sea and ports.

The EMOA-SSR algorithm was launched for each combination of the PF size and number of linear secant segments. Moreover, three replications were performed to estimate the average values of computational time. The results of the time complexity analysis are depicted in Fig. 7 and more details are reported in Table 3. The objective function values at the PF solutions are not reported for the considered scenarios, since no significant changes in the objective function values at the PF solutions (i.e., less than 0.24%) were observed after increasing the number of secant segments in the approximating bunker fuel consumption function beyond four segments. It can be observed that the EMOA-SSR algorithm is much more sensitive to the number of linear secant segments used in the approximation for the bunker fuel consumption function compared to the desired number of PF points. In particular, substantial increases in the computational time were recorded after increasing the number of linear secant segments used in the piecewise approximating function. However, based on the previously conducted analysis (see Fig. 4), the piecewise approximating function with four linear secant segments provides a precise approximation of the bunker fuel consumption function. Hence, the EMOA-SSR algorithm with four linear secant segments and twenty PF points was further used to obtain the managerial insights as a part of the conducted computational experiments.

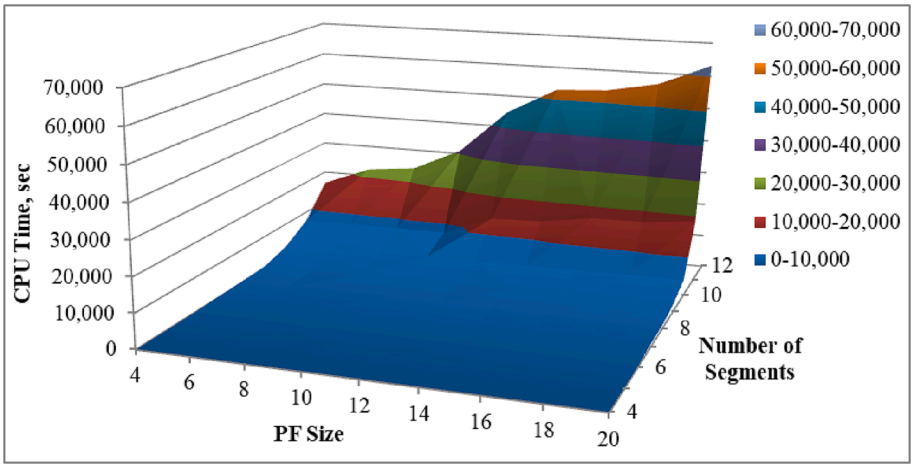

Fig. 7. Time complexity analysis results for the EMOA-SSR algorithm.

Table 3
Average EMOA-SSR computational time for the considered scenarios (reported in seconds).

$\|K\|\backslash\|PF\|$	4	6	8	10	12	14	16	18	20
4	8.90	11.88	19.20	21.34	31.10	38.21	39.46	108.51	113.48
5	19.21	23.16	34.66	74.15	91.32	100.70	105.80	120.17	148.01
6	47.57	67.31	82.49	112.17	131.05	171.84	175.91	183.88	196.89
7	179.88	224.36	309.73	333.97	365.21	394.80	710.71	812.19	869.34
8	322.64	345.21	502.64	688.00	789.51	851.77	910.29	940.99	966.18
9	513.10	653.21	1,260.24	1,301.42	1,372.73	1,893.03	1,959.05	2,078.14	2,153.38
10	2,776.58	2,876.02	3,227.05	3,965.16	4,093.93	4,314.49	4,432.99	4,777.40	4,852.13
11	7,234.02	7,450.32	7,492.46	7,520.00	13,618.11	14,217.11	16,667.28	16,921.64	18,611.06
12	16,268.32	22,160.84	23,791.07	30,892.82	44,757.27	52,911.45	53,709.32	56,605.57	63,148.06

6.3. Managerial implications

This section of the manuscript describes the managerial implications derived from the solutions obtained for the **MOSSR-2** mathematical model. In particular, the solutions derived at the corner PF points were thoroughly analyzed. Additionally, several sensitivity analyses were carried out for various disruption scenarios to assess their impact on the selected ship schedule recovery options. The supplementary set of sensitivity analyses examined the effects of changes in the unit fuel cost on the decision variables of the **MOSSR-2** mathematical model. Twenty problem instances were generated to reveal the managerial implications by changing the originally planned ship arrival time ($\tau_p^{arr}, p \in P$ – hours) at each port of the EPIC shipping route as follows: $\tau_{p+1}^{arr} = \tau_p^{arr} + (d_p^{leg}/s_p) \forall p \in P$ – hours, where $d_p^{leg}, p \in P$ – length of voyage leg p (nmi); and $s_p = U[15;18] \forall p \in P$ – sailing speed of ships based on the originally planned schedule (knots).

6.3.1. Analysis of the solutions at the corner Pareto Front points

The first analysis aimed to conduct a detailed evaluation of the corner PF solutions (i.e., the solutions that yield the minimum total late ship arrivals at ports [F_1^*] and the solutions that yield the minimum total profit loss [F_2^*]). The EMOA-SSR algorithm was executed for all the considered problem instances and the base disruption scenario with disruptive incidents at sea and ports. The following information was collected for the recovered ship schedules at the corner PF points: (1) the value of F_1 objective; (2) the value of F_2 objective; (3) the average sailing speed adjustment of ships weighted by the length of voyage legs – $\Delta^{sea-w} = (\sum_{p\in P} d_p^{leg} \bullet \Delta_p^{sea})/(\sum_{p\in P} d_p^{leg})$; (4) the average sailing speed of ships weighted by the length of voyage legs – $\overline{s^w} = (\sum_{p\in P} d_p^{leg} \bullet \overline{s_p})/(\sum_{p\in P} d_p^{leg})$; (5) the total sailing time – $\overline{\tau^{sail}} = \sum_{p\in P} \overline{\tau_p^{sail}}$; (6) the total waiting time – $\overline{\tau^{wait}} = \sum_{p\in P} \overline{\tau_p^{wait}}$; (7) the total handling time – $\overline{\tau^{hand}} = \sum_{p\in P} \overline{\tau_p^{hand}}$; (8) the total turnaround time – $\overline{STT}$; (9) the total bunker fuel consumption – $\overline{FC} = \sum_{p\in P} \sum_{k\in K} \overline{FC_{pk}}$; (10) the total number of skipped ports – $x^{skip} = \sum_{p\in P} x_p^{skip}$; (11) the total number of container diversion moves – $x^{div} = \sum_{p\in P} \sum_{p^*\in P} x_{pp^*}^{div}$; (12) the total number of diverted containers – $d^{div} = \sum_{p\in P} \sum_{p^*\in P} d_{pp^*}^{div}$; and (13) total number of containers on board the ships over all voyage legs – $d^{sea} = \sum_{p\in P} d_p^{sea}$.

The relative changes in the mean values of all the considered variables over the twenty problem instances were calculated by comparing

Table 4
Analysis of the solutions at the corner PF points for the considered problem instances.

F_1^* Corner Point Instance	F_1, hours	F_2, 10^6 USD	Δ^{sea-w}, knots	$\overline{s^w}$, knots	$\overline{\tau^{sail}}$, hours	$\overline{\tau^{wait}}$, hours	$\overline{\tau^{hand}}$, hours	$\overline{STT}$, hours	$\overline{FC}$, tons	x^{skip}	x^{div}	d^{div}, TEUs	d^{sea}, TEUs
1	209.37	30.00	4.73	21.56	811.73	0.00	90.76	902.48	2,516.90	3	1	513	57,211
2	248.17	30.00	4.24	21.07	830.54	1.00	90.78	922.31	2,067.69	3	1	513	56,698
3	51.34	30.00	2.93	19.76	885.56	17.62	96.19	999.37	2,359.57	3	1	513	56,698
4	93.93	30.00	4.48	21.32	821.13	0.00	83.25	904.37	2,196.84	3	1	513	56,698
5	160.76	30.00	4.28	21.11	829.08	42.44	88.35	959.87	2,320.21	3	1	513	57,211
6	119.56	30.00	4.53	21.36	819.32	12.57	94.72	926.61	2,253.17	3	1	513	56,698
7	238.43	30.00	4.94	21.77	804.04	13.69	90.76	908.48	2,516.90	3	1	513	57,211
8	84.20	30.00	4.16	20.99	833.68	6.55	77.04	917.26	2,128.76	3	1	513	57,211
9	70.17	30.00	4.07	20.90	837.54	7.47	87.47	932.48	2,422.05	3	1	513	57,211
10	69.33	30.00	4.28	21.12	828.91	13.09	94.72	936.73	2,253.17	3	1	513	56,698
11	364.84	30.00	4.62	21.45	815.85	15.79	92.74	924.37	2,455.46	3	1	513	56,698
12	308.20	30.00	4.86	21.69	806.95	0.00	92.24	899.19	2,207.85	3	1	513	56,698
13	210.96	30.00	4.22	21.05	831.39	43.26	94.72	969.37	2,253.17	3	1	513	56,698
14	175.75	30.00	4.10	20.93	836.09	1.00	91.27	928.36	2,315.30	3	1	513	56,698
15	283.54	30.00	3.92	20.75	843.50	13.49	89.65	946.64	2,113.00	3	1	513	56,698
16	115.16	30.00	4.91	21.75	804.91	1.00	80.16	886.07	2,220.03	3	1	513	56,698
17	360.15	30.00	4.48	21.31	821.20	5.00	97.31	923.51	2,348.02	3	1	513	56,698
18	276.61	30.00	4.15	20.98	834.18	0.00	89.65	923.84	2,113.00	3	1	513	56,698
19	383.23	30.00	5.35	22.19	788.92	1.00	90.92	880.84	2,359.92	3	1	513	57,211
20	169.20	30.00	4.22	21.05	831.52	1.94	91.27	924.73	2,315.30	3	1	513	56,698
Mean	**199.65**	**30.00**	**4.37**	**21.21**	**825.80**	**9.84**	**90.20**	**925.85**	**2,286.81**	**3**	**1**	**513**	**56,851**
F_2^* Corner Point Instance	F_1, hours	F_2, 10^6 USD	Δ^{sea-w}, knots	$\overline{s^w}$, knots	$\overline{\tau^{sail}}$, hours	$\overline{\tau^{wait}}$, hours	$\overline{\tau^{hand}}$, hours	$\overline{STT}$, hours	$\overline{FC}$, tons	x^{skip}	x^{div}	d^{div}, TEUs	d^{sea}, TEUs
1	2,500	4.70	1.09	17.92	976.84	0.00	419.71	1,396.55	1,626.56	0	0	0	57,622
2	2,500	4.61	1.16	17.99	972.68	0.00	429.87	1,402.55	1,640.93	0	0	0	57,622
3	2,500	4.36	0.19	17.02	1,028.12	1.00	433.85	1,462.98	1,368.83	0	0	0	57,622
4	2,500	4.60	1.31	18.15	964.61	1.00	433.85	1,399.46	1,655.60	0	0	0	57,622
5	2,500	4.45	0.60	17.43	1,004.33	0.00	433.85	1,438.18	1,484.86	0	0	0	57,622
6	2,500	4.59	1.10	17.93	976.03	1.00	429.87	1,406.90	1,631.50	0	0	0	57,622
7	2,500	4.67	1.66	18.49	946.65	0.00	429.87	1,376.52	1,710.24	0	0	0	57,622
8	2,500	4.68	1.09	17.92	976.86	1.00	423.69	1,401.55	1,626.49	0	0	0	57,622
9	2,500	4.57	1.08	17.91	977.19	1.00	433.85	1,412.04	1,624.45	0	0	0	57,622
10	2,500	4.46	0.65	17.48	1,001.22	0.00	433.85	1,435.07	1,497.05	0	0	0	57,622
11	2,500	4.73	1.35	18.18	962.84	0.00	419.71	1,382.55	1,662.14	0	0	0	57,622
12	2,500	4.83	1.54	18.37	952.87	1.00	415.48	1,369.35	1,698.56	0	0	0	57,622
13	2,500	4.48	0.69	17.52	998.88	0.00	433.85	1,432.73	1,517.46	0	0	0	57,622
14	2,500	4.73	1.34	18.17	963.06	1.00	419.71	1,383.77	1,662.21	0	0	0	57,622
15	2,500	4.69	1.07	17.90	977.81	0.00	419.71	1,397.52	1,620.66	0	0	0	57,622
16	2,500	4.72	1.32	18.15	964.38	1.00	419.71	1,385.09	1,652.74	0	0	0	57,622
17	2,500	4.74	1.41	18.24	959.58	1.00	419.71	1,380.29	1,674.08	0	0	0	57,622
18	2,500	4.74	1.40	18.23	960.11	1.00	419.71	1,380.82	1,669.97	0	0	0	57,622
19	2,500	4.91	1.83	18.66	937.84	1.00	411.15	1,349.99	1,748.11	0	0	0	57,622
20	2,500	4.57	1.09	17.92	976.54	1.00	433.85	1,411.40	1,621.63	0	0	0	57,622
Mean	**2,500**	**4.64**	**1.15**	**17.98**	**973.92**	**0.60**	**425.74**	**1,400.27**	**1,619.70**	**0**	**0**	**0**	**57,622**

the corner point F_1^* to the corner point F_2^* (see Table 4). Since the corner point F_1^* has the optimum value for the objective function F_1, the mean value of F_1 at the corner point F_1^* (199.65 h) was 92.01% lower than that of at the corner point F_2^* (2,500 h). On the other hand, the second objective function F_2 has the lowest value at the corner point F_2^*, so the mean value of F_2 at the corner point F_2^* (4.64×10^6 USD) was 84.53% lower than that of at the corner point F_1^* (30×10^6 USD). The mean values for Δ^{sea-w} (the average sailing speed adjustment of ships weighted by the length of voyage legs) and $\overline{s^w}$ (the average sailing speed of ships weighted by the length of voyage legs) were both found to be significantly lower at the corner point F_2^* than those of at corner point F_1^*. Such results can be explained by the fact that the shipping line chose the sailing speed adjustment option and sail at higher speeds in order to minimize the total ship late arrivals at ports and reach the best value for F_1 (i.e., the corner point F_1^*). On the contrary, if more emphasis is given to the total profit loss minimization (i.e., the corner point F_2^*), the shipping line had to use the sailing speed adjustment option on a limited basis to reduce the associated bunker fuel costs. Indeed, the bunker fuel consumption values were on average 41.19% lower at the corner point F_2^* compared to the corner point F_1^*. Moreover, the relative difference between the mean values of total sailing time and total turnaround time at the corner point F_1^* and the corner point F_2^* were found to be −15.21% and –33.88%, respectively.

Some interesting insights were also revealed for x^{skip} (port skipping decision variable). Port skipping was found to be a common option for the F_1^* ship schedules mainly due to the fact that the objective function F_1 is solely focused on the minimization of total ship late arrivals at ports without considering the costs that are associated with the port skipping decision. As a result, the mean value for the total handling time at the corner point F_1^* was found to be 78.81% lower than that of at the corner point F_2^*, which confirms the wide implementation of the port skipping option at the corner point F_1^* to offset the delays due to disruptive incidents.

Furthermore, port skipping with the diversion of containers was identified to be a more popular option for the F_1^* ship schedules compared to the F_2^* ship schedules, since the container diversion costs are not captured directly by the objective function F_1. The computational experiments also show a more substantial deviation in the total number of containers on board the ships over all voyage legs for the F_1^* ship schedules compared to the F_2^* ship schedules, which can be explicated by port skipping and container diversion decisions. Based on the conducted analysis, it can be concluded that the proposed multi-objective optimization model for ship schedule recovery can effec-

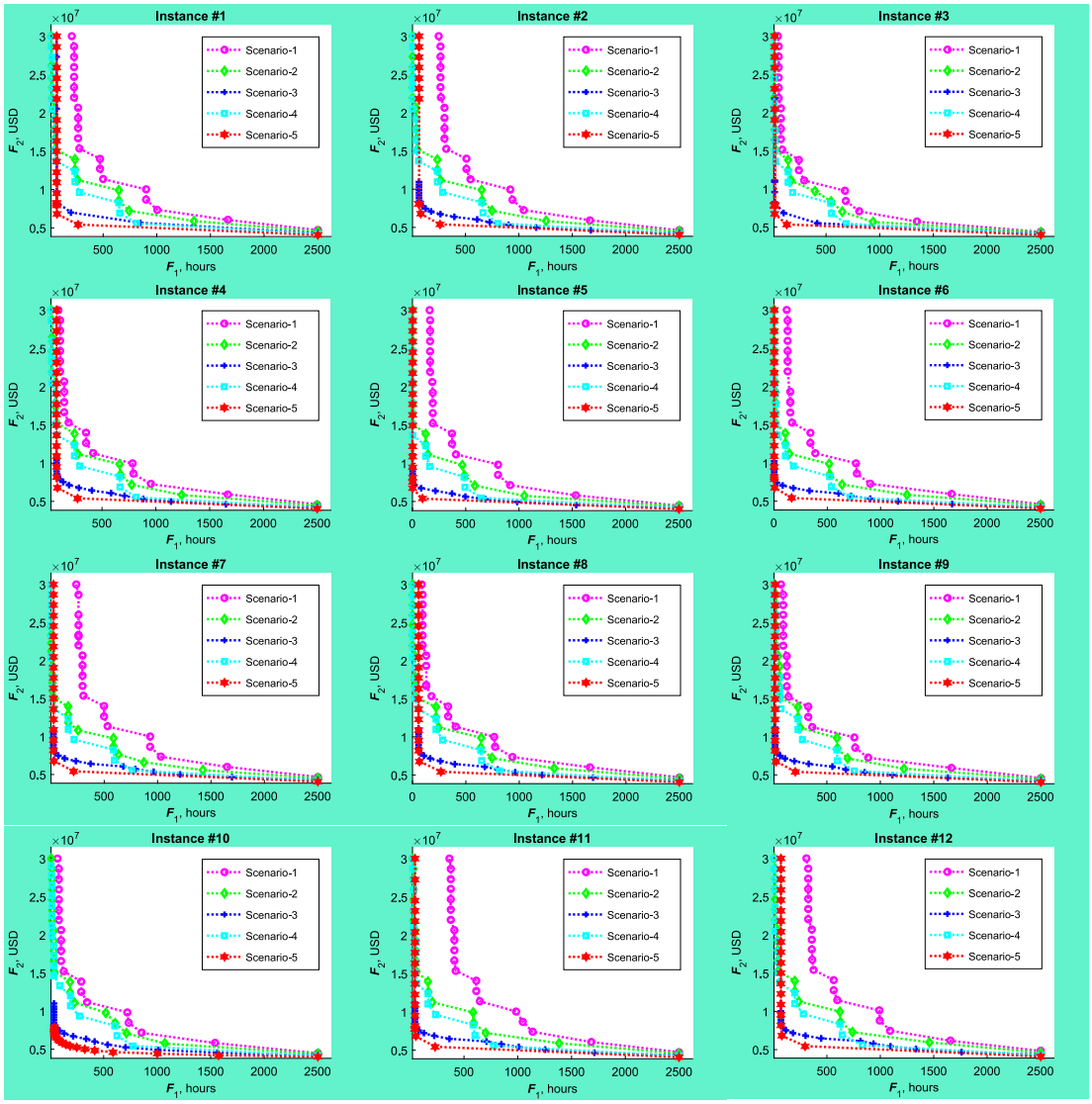

Fig. 8. Pareto Fronts obtained for the considered disruption type scenarios and problem instances “1” through “12”.

tively assist shipping lines with the analysis of various schedule recovery options under competing objectives.

6.3.2. Sensitivity analysis for the disruption types

The second analysis aimed to determine the impacts of disruption types on ship schedule recovery under multi-objective settings. A total of five scenarios of disruption types were considered, including the following: (1) disruptive incidents occur at sea and ports (i.e., the base scenario); (2) disruptive incidents occur at ports only (i.e., disruptions at the Ports of Qasim, Rotterdam, and Bremerhaven); (3) disruptive incidents occur at the port early in the voyage (i.e., disruption at the Port of Qasim); (4) disruptive incidents occur at the ports later in the voyage (i.e., disruptions at the Port of Rotterdam and the Port of Bremerhaven); and (5) no disruptive incidents occur throughout the ship voyage. More details regarding the considered scenarios of disruptive incidents and their effects are provided in Section 6.1 of the manuscript. The adopted EMOA-SSR algorithm was executed for all the disruption type scenarios and all the considered problem instances. The obtained PFs are illustrated in Fig. 8 for the problem instances "1" through "12", but similar patterns were noticed for the remaining problem instances.

It can be observed that the obtained PFs vary substantially for different disruption types. As expected, the PFs with the largest total port arrival delays and total profit loss were recorded for the scenario when disruptive incidents were reported at sea and ports (i.e., the base scenario). Substantial total port arrival delays and total profit loss were also determined for the scenario with disruptive incidents at ports only (i.e., scenario "2"). However, it is anticipated that the total port arrival delays and total profit loss would be even larger without the implementation of ship schedule recovery options, which were proposed in this study (i.e., port skipping without the diversion of containers to alternative ports, port skipping with the diversion of containers to alternative ports, increasing ship sailing speeds at specific voyage legs, and increasing ship handling rates at specific ports).

Furthermore, throughout the computational experiments, the impacts of disruption types on sailing speed, port handling time, port skipping, and container diversion decisions were analyzed, and the results are presented in Table 5 for all the obtained PF points and problem instance "1", but similar patterns were noticed for the remaining problem instances. Lower ship sailing speeds were generally observed for the scenario with disruptive incidents reported at sea and ports. Such a finding can be explained by the fact that the shipping line was only able to partially offset the delays due to disruptions at sea and ports by implementing the sailing speed adjustment recovery strategy (i.e., the desirable sailing speed level was not achieved even after increasing sailing speed). The handling rate selection was mainly governed by the delay and financial perspectives, not by the types of disruptions (see Table 5). More specifically, if the objective was to minimize the total profit loss (the best solution for which corresponds to PF#1 representing the F_2^* ship schedule), the shipping line generally requested lower handling rates for all the disruption scenarios to avoid additional

Table 5
Analysis of sailing speed, port handling time, port skipping, and container diversion decisions for all the PF points obtained for problem instance "1".

PF#	**Weighted Sailing Speed (knots)**					**Total Port Handling Time (hours)**				
	Scenario 1	Scenario 2	Scenario 3	Scenario 4	Scenario 5	Scenario 1	Scenario 2	Scenario 3	Scenario 4	Scenario 5
1	17.92	18.26	17.38	16.84	15.85	419.71	433.85	320.33	368.33	241.33
2	18.35	21.78	22.23	21.55	21.49	349.26	373.40	264.72	311.74	193.74
3	20.42	22.48	22.01	22.02	22.10	272.63	301.03	183.13	263.65	140.16
4	20.75	22.08	22.52	21.34	22.56	240.93	260.01	139.54	232.42	95.41
5	20.36	21.92	22.46	22.38	23.14	224.86	253.61	95.66	204.13	95.41
6	20.84	21.93	21.99	21.86	23.14	175.99	185.08	92.53	174.78	95.41
7	20.93	21.83	22.67	21.91	23.14	157.79	158.39	92.53	177.26	95.41
8	20.73	21.99	22.69	21.83	23.14	157.79	148.41	95.27	140.06	95.41
9	20.84	22.04	22.67	22.54	23.14	123.27	137.88	92.53	96.18	95.41
10	20.75	21.83	22.72	21.76	23.14	113.23	127.98	99.06	119.60	95.41
11	20.75	20.90	22.72	21.51	23.14	113.23	94.58	99.06	116.99	95.41
12	20.67	21.77	22.72	21.86	23.14	109.94	127.98	99.06	131.48	95.41
13	20.75	21.91	22.72	21.53	22.71	113.23	136.54	99.06	118.96	102.48
14	20.75	21.58	22.72	21.61	23.14	101.31	121.14	99.06	122.05	95.41
15	20.75	21.58	22.72	21.53	23.14	101.31	121.14	99.06	118.36	95.41
16	20.81	21.75	22.72	21.51	23.14	97.93	127.44	99.06	118.36	95.41
17	20.76	22.24	22.72	21.35	23.14	97.93	86.24	99.06	110.98	95.41
18	20.24	20.54	22.72	21.61	23.44	79.82	79.91	99.06	121.95	95.41
19	20.55	20.66	22.72	21.41	23.14	86.03	79.82	99.06	81.86	95.41
20	21.56	21.53	22.72	22.70	23.39	90.76	76.17	99.06	72.24	95.41
PF#	**Total Number of Skipped Ports**					**Total Number of Container Diversion Moves**				
	Scenario 1	Scenario 2	Scenario 3	Scenario 4	Scenario 5	Scenario 1	Scenario 2	Scenario 3	Scenario 4	Scenario 5
1	0	0	0	0	0	0	0	0	0	0
2	1	0	0	0	0	1	0	0	0	0
3	1	1	1	0	0	1	1	1	0	0
4	1	1	1	0	0	1	1	1	0	0
5	1	1	1	1	0	1	1	1	1	0
6	2	2	1	1	0	2	2	0	1	0
7	2	2	1	1	0	2	2	0	1	0
8	2	2	1	2	0	2	2	1	2	0
9	3	3	1	2	0	3	3	0	2	0
10	3	3	1	2	0	3	3	0	2	0
11	3	3	1	2	0	3	3	0	2	0
12	3	3	1	2	0	3	3	0	2	0
13	3	3	1	2	0	3	2	0	1	0
14	3	3	1	2	0	2	2	0	1	0
15	3	3	1	2	0	2	2	0	1	0
16	3	3	1	2	0	2	2	0	1	0
17	3	3	1	2	0	2	2	0	1	0
18	3	3	1	2	0	1	1	0	1	0
19	3	3	1	2	0	2	1	0	0	0
20	3	3	1	2	0	1	1	0	0	0

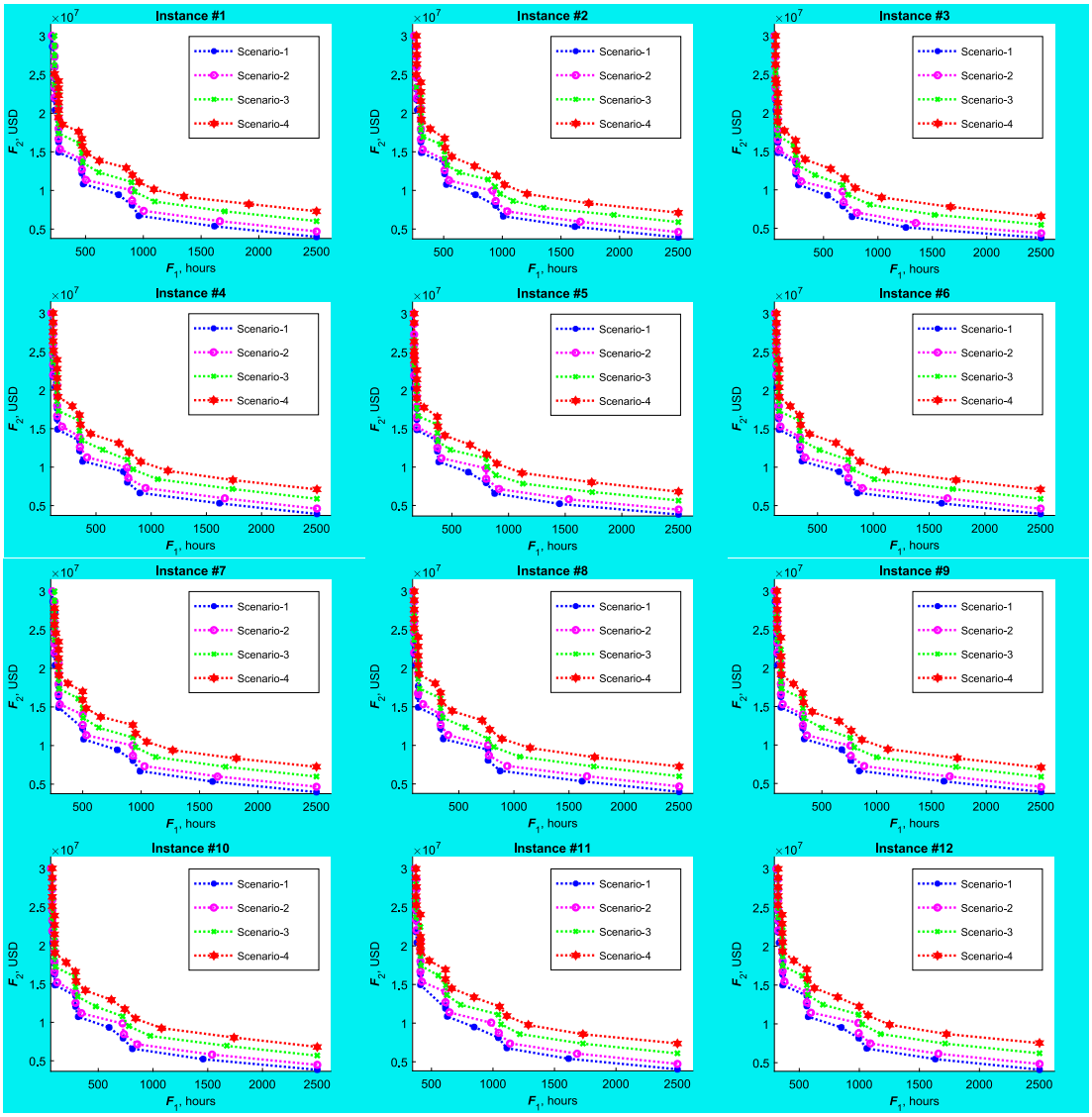

Fig. 9. Pareto Fronts obtained for the considered unit fuel cost scenarios and problem instances "1" through "12".

container handling costs at ports. On the contrary, if the objective was to minimize the total late ship arrivals at ports (the best solution for which corresponds to PF#20 representing the F_1^* ship schedule), the shipping line generally requested higher handling rates for all the disruption scenarios to better offset the disruption effects regardless of additional container handling costs at ports.

The port skipping and container diversion recovery strategies were mainly used for the first two disruption scenarios (i.e., disruptive incidents occur at sea and ports and disruptive incidents occur at ports only), when the objective was to minimize the total late ship arrivals at ports (see Table 5). Fewer port skipping and container diversion moves were recorded for the scenario without disruptions and for the scenarios with limited disruptions (e.g., disruptive incidents occur at only one port early in the voyage). Such a finding confirms that the port skipping and container diversion recovery strategies can be effective to offset the impacts of major disruptions. These recovery strategies are generally not used for the cases with minor disruptions mainly due to the costs associated with port skipping and handling of the diverted demand. Based on the conducted analysis, it can be concluded that the proposed multi-objective optimization model and the EMOA-SSR algorithm can effectively assist shipping lines with the analysis of impacts from different disruption types and selection of the appropriate recovery options.

6.3.3. *Sensitivity analysis for the unit fuel cost*

The third analysis aimed to determine the impacts of unit fuel cost values on ship schedule recovery under multi-objective settings. A total of four scenarios for the unit fuel cost values were considered, including the following: (1) VLSFO = 400 USD/ton and ULSFO = 600 USD/ton (i.e., a 50% reduction in the unit fuel prices compared to the base scenario); (2) VLSFO = 800 USD/ton and ULSFO = 1,200 USD/ton (i.e., the base scenario); (3) VLSFO = 1,600 USD/ton and ULSFO = 2,400 USD/ton (i.e., a 100% increase in the unit fuel prices compared to the base scenario); and (4) VLSFO = 2,400 USD/ton and ULSFO = 3,600 USD/ton (i.e., a 200% increase in the unit fuel prices compared to the base scenario). The adopted EMOA-SSR algorithm was executed for all the unit fuel cost scenarios, all the considered problem instances, and the base disruption scenario with disruptive incidents at sea and ports. The obtained PFs are illustrated in Fig. 9 for the problem instances "1" through "12", but similar patterns were noticed for the remaining problem instances. Furthermore, the average values of ship sailing speed weighted by the length of voyage legs were estimated throughout the experiments and are presented in Fig. 10 for the considered unit fuel cost scenarios and problem instances. Note that Fig. 10 shows the information for the F_2^* corner point only, since the unit fuel cost is not included in the F_1 objective function directly (hence, no clear patterns were identified for

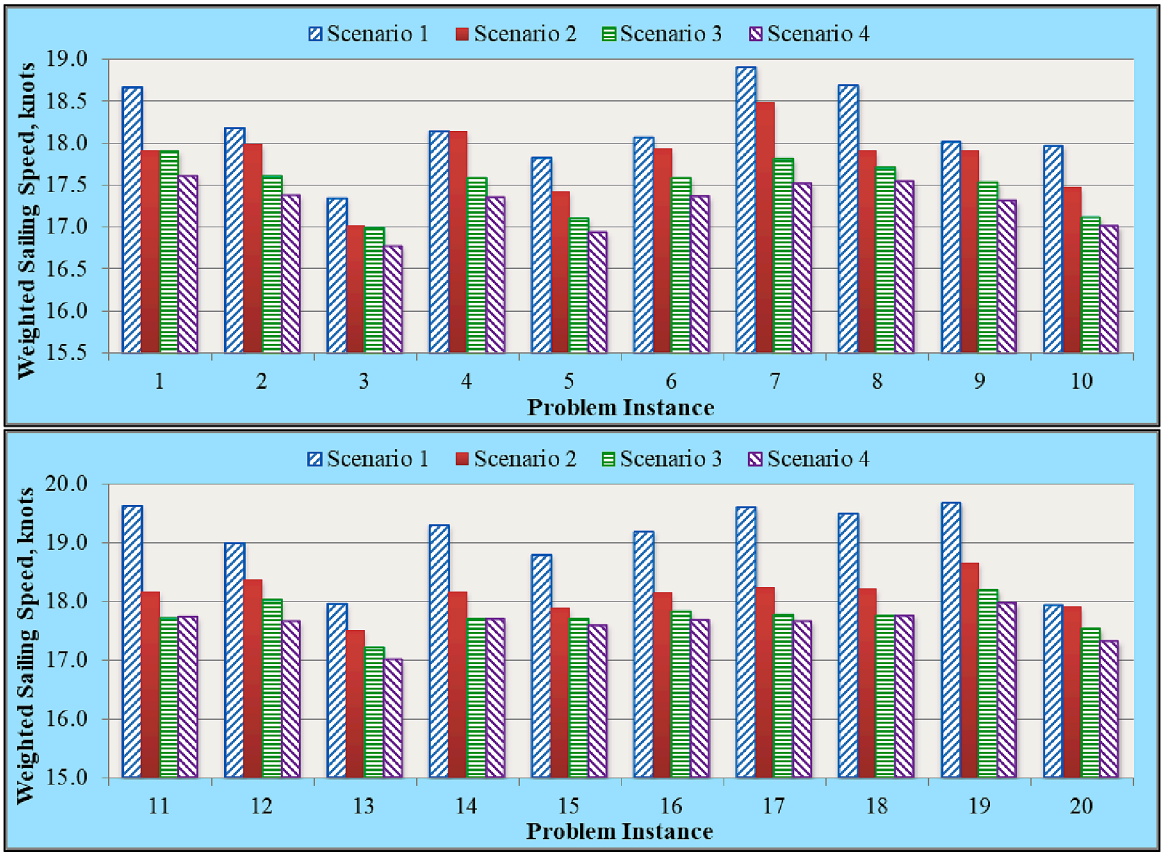

Fig. 10. Average weighted ship sailing speed values for the considered fuel cost scenarios and problem instances.

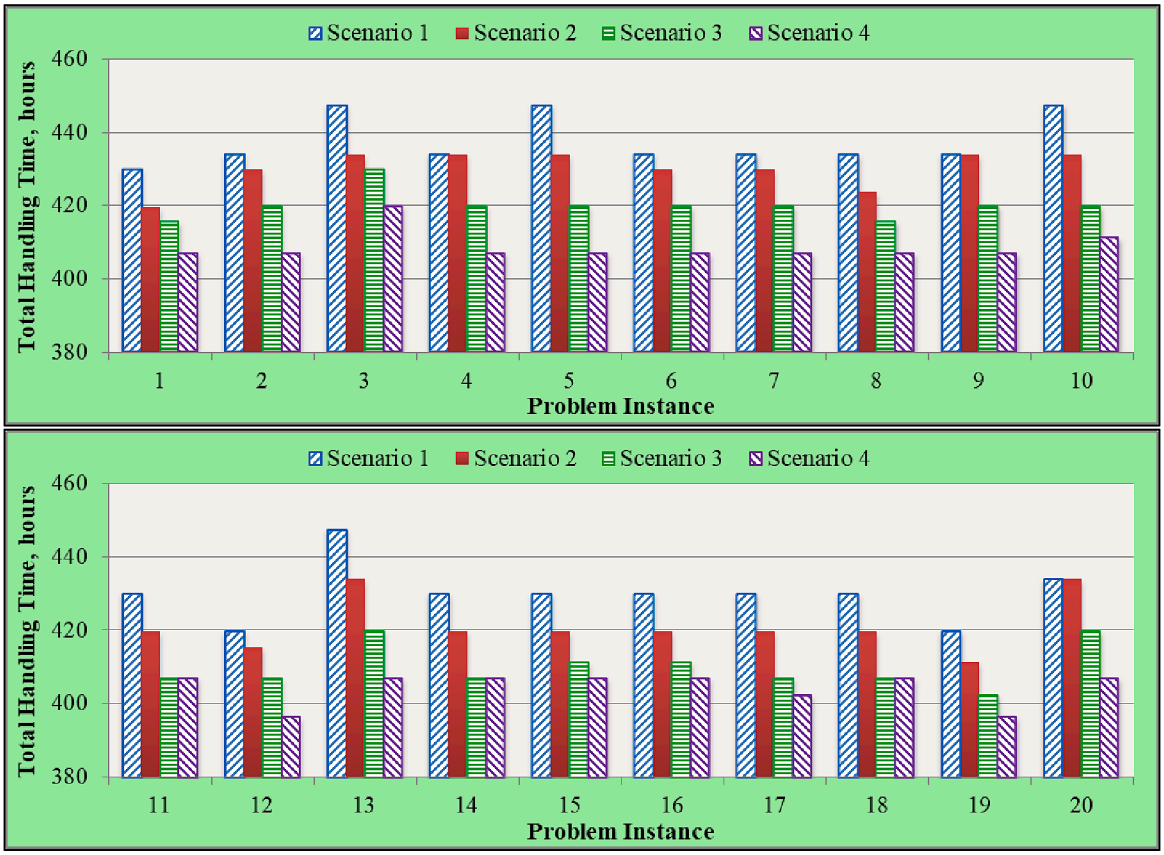

Fig. 11. Total port handling time values for the considered fuel cost scenarios and problem instances.

the F_1^* corner point solutions after changing the values of the unit fuel cost).

It can be observed that inferior PFs were generally obtained for the scenarios with higher unit fuel cost. Such results can be justified by the fact that higher bunker fuel consumption costs increase the total profit loss. When the unit fuel cost was fairly low (e.g., scenario "1"), the shipping line used the ship sailing speed adjustment option for the majority of the considered problem instances to offset the delays caused by disruptive incidents throughout the voyage (see Fig. 10). However, the ship sailing speed adjustment option will not be an effective strategy and cannot be used to the same extent for the scenarios with high unit fuel cost, which can be confirmed by lower ship sailing speeds recorded for the scenarios with high unit fuel cost. The conducted computational experiments also show that an increase in the unit fuel cost impacted the selection of handling rates at ports of call (see Fig. 11). In particular, an increase in the unit fuel cost prompted the shipping line selecting higher handling rates at ports of call, which caused a reduction in the total port handling time. Therefore, the handling rate adjustment recovery strategy became preferential over the sailing speed adjustment strategy for the scenarios with high unit fuel costs. No changes in port skipping decisions and container diversion moves were observed after changing the unit fuel cost. Based on the conducted analysis, it can be concluded that the proposed multi-objective optimization model and the EMOA-SSR algorithm can effectively assist shipping lines with the analysis of impacts from unit fuel cost changes and selection of the appropriate recovery options, which can be viewed as critical considering the existing uncertainties on the energy market.

7. Concluding remarks and future research

Liner shipping and maritime transportation in general play a critical role for supply chain management. However, different unexpected events can disrupt liner shipping services. The rescheduling of original ship operations would be necessary to counteract the negative effects of such disruptions. Different ship schedule recovery options can be adopted in response to disruptive incidents. However, shipping lines face conflicting decisions when selecting ship schedule recovery options (e.g., the ship speeding-up option could effectively reduce delays during the voyage but would increase the fuel cost). Nevertheless, there is a lack of analytical methods that enable the evaluation of competing objectives in ship schedule recovery and effective multi-objective solution approaches. Therefore, this study proposed a new type of the multi-objective mathematical formulation for ship schedule recovery that aims not only to minimize the total late ship arrivals at ports but also to minimize the total profit loss due to disruptive incidents that may occur at sea and/or at ports. An exact optimization algorithm was adopted to obtain optimal Pareto Fronts.

The computational experiments that were conducted for the EPIC (Europe Pakistan India Consortium) shipping route demonstrated that the proposed exact optimization algorithm is able to generate Pareto Fronts in a timely manner. The results also showed that port skipping and port skipping with the diversion of containers were popular ship schedule recovery options when more emphasis was given to the total delay minimization objective. Furthermore, it was found that port skipping and container diversion decisions could cause substantial fluctuations in the total number of containers transported on board the ships. The conducted sensitivity analyses showcased that the port arrival delays and total profit losses could be significantly affected by the nature of disruptive incidents throughout the ship voyage. Moreover, the ship sailing speed adjustment option might not be an effective strategy for the scenarios with high unit fuel cost, and shipping lines could incur lower financial losses by using alternative schedule recovery options or even enduring the delays caused by disruptive incidents. It can be concluded that the proposed multi-objective optimization model for ship schedule recovery and the presented exact optimization algorithm can effectively assist shipping lines with the analysis of various schedule recovery options under competing objectives.

Based on the outcomes of this study, several future research opportunities were identified. First, more emphasis should be given to the development of novel forecasting methods to accurately predict the frequency and duration of disruptive incidents. Second, the accuracy of bunker fuel consumption modeling could be enhanced by incorporating additional relevant factors, including but not limited to ship age, ship size, and history of previous maintenance activities. Third, alternative measures should be considered to further improve environmental sustainability of liner shipping services under normal and disruptive operational conditions (e.g., installation of scrubbers). Fourth, the proposed multi-objective exact optimization algorithm could be evaluated against alternative methods (e.g., common types of multi-objective metaheuristic algorithms, decomposition methods applied in multi-objective settings, and relaxation techniques). Fifth, this study assumed that the cargo can be diverted from a skipped port that experienced a disruption to one alternative port. The future research could explore different cargo diversion options, where the cargo can be diverted to multiple alternative ports based on their port handling and inland transportation capacity. Last but not least, collaborative opportunities among alliance partners can be explored further to better respond to different types of disruptive incidents in liner shipping services.

CRediT authorship contribution statement

Zeinab Elmi: Conceptualization, Methodology, Data curation, Investigation, Writing – original draft. **Bokang Li:** Methodology, Data curation, Investigation, Writing – original draft. **Benbu Liang:** Methodology, Data curation, Investigation, Writing – original draft. **Yui-yip Lau:** Methodology, Data curation, Investigation, Writing – original draft. **Marta Borowska-Stefańska:** Methodology, Data curation, Investigation, Writing – original draft. **Szymon Wiśniewski:** Methodology, Data curation, Investigation, Writing – original draft. **Maxim A. Dulebenets:** Conceptualization, Methodology, Data curation, Visualization, Investigation, Writing – original draft, Writing – review & editing.

Declaration of Competing Interest

The authors declare that they have no known competing financial interests or personal relationships that could have appeared to influence the work reported in this paper.

Data availability

Data will be made available on request.

References

Abioye, O. F., Dulebenets, M. A., Kavoosi, M., Pasha, J., & Theophilus, O. (2021). Vessel schedule recovery in liner shipping: Modeling alternative recovery options. *IEEE Transactions on Intelligent Transportation Systems, 22*(10), 6420–6434.

Abioye, O. F., Dulebenets, M. A., Pasha, J., & Kavoosi, M. (2019). A vessel schedule recovery problem at the liner shipping route with emission control areas. *Energies, 12*(12), 2380.

Agcs Safety and Shipping Review 2022 https://www.agcs.allianz.com/news-and-insights/reports/shipping-safety.html 2022 Available at: Accessed: 17 October 2022.

Alharbi, A., Wang, S., & Davy, P. (2015). Schedule design for sustainable container supply chain networks with port time windows. *Advanced Engineering Informatics, 29*(3), 322–331.

Asghari, M., Jaber, M. Y., & Mirzapour Al-e-hashem, S. M. J. (2022). Coordinating vessel recovery actions: Analysis of disruption management in a liner shipping service. *European Journal of Operational Research.*

Brouer, B. D., Dirksen, J., Pisinger, D., Plum, C. E., & Vaaben, B. (2013). The Vessel Schedule Recovery Problem (VSRP)–A MIP model for handling disruptions in liner shipping. *European Journal of Operational Research, 224*(2), 362–374.

Brouer, B. D., Karsten, C. V., & Pisinger, D. (2017). Optimization in liner shipping. *4OR, 15*(1), 1–35.

Cheraghchi, F., Abualhaol, I., Falcon, R., Abielmona, R., Raahemi, B., & Petriu, E. (2017). Big-data-enabled modelling and optimization of granular speed-based vessel schedule recovery problem. In *In 2017 IEEE International Conference on Big Data (Big Data)* (pp. 1786–1794). IEEE.

Cheraghchi, F., Abualhaol, I., Falcon, R., Abielmona, R., Raahemi, B., & Petriu, E. (2018). Modeling the speed-based vessel schedule recovery problem using evolutionary multiobjective optimization. *Information Sciences, 448*, 53–74.

Cheraghchi, F., Abualhaol, I., Falcon, R., Abielmona, R., Raahemi, B., & Petriu, E. (2020). Distributed Multi-Objective Cooperative Coevolution Algorithm for Big-Data-Enabled Vessel Schedule Recovery Problem. In *2020 IEEE Conference on Cognitive and Computational Aspects of Situation Management (CogSIMA)* (pp. 90–97). IEEE.

Chuang, T. N., Lin, C. T., Kung, J. Y., & Lin, M. D. (2010). Planning the route of container ships: A fuzzy genetic approach. *Expert Systems with Applications, 37*(4), 2948–2956.

Clausen, J., Larsen, A., Larsen, J., & Rezanova, N. J. (2010). Disruption management in the airline industry—Concepts, models and methods. *Computers & Operations Research, 37*(5), 809–821.

CMA CGM. Europe Pakistan India Consortium https://www.cma-cgm.fr/produits-services/lignes-maritimes/flyer/EPIC 2022 Available at: Accessed: 18 October 2022.

Dadashi, A., Dulebenets, M. A., Golias, M. M., & Sheikholeslami, A. (2017). A novel continuous berth scheduling model at multiple marine container terminals with tidal considerations. *Maritime Business Review, 2*(2), 142–157.

De, A., Wang, J., & Tiwari, M. K. (2021). Fuel bunker management strategies within sustainable container shipping operation considering disruption and recovery policies. *IEEE Transactions on Engineering Management, 68*(4), 1089–1111.

Ding, J., & Xie, C. (2022). Stochastic Programming for Liner Ship Routing and Scheduling under Uncertain Sea Ice Conditions in the Northern Sea Route. *Transportation Research Record, 2676*(1), 38–53.

Du, W., Li, Y., Zhang, G., Wang, C., Zhu, B., & Qiao, J. (2022b). Ship weather routing optimization based on improved fractional order particle swarm optimization. *Ocean Engineering, 248*, Article 110680.

Du, Y., Meng, Q., & Wang, Y. (2015). Budgeting fuel consumption of container ship over round-trip voyage through robust optimization. *Transportation Research Record, 2477*(1), 68–75.

Du, J., Zhao, X., Guo, L., & Wang, J. (2022a). Machine Learning-Based Approach to Liner Shipping Schedule Design. *Journal of Shanghai Jiaotong University (Science), 27*(3), 411–423.

Du, W., Li, Y., Zhang, G., Wang, C., Chen, P., & Qiao, J. (2021). Estimation of ship routes considering weather and constraints. *Ocean Engineering, 228*, Article 108695.

Dulebenets, M. A. (2018). A comprehensive multi-objective optimization model for the vessel scheduling problem in liner shipping. *International Journal of Production Economics, 196*, 293–318.

Dulebenets, M. A., Pasha, J., Abioye, O. F., & Kavoosi, M. (2021). Vessel scheduling in liner shipping: A critical literature review and future research needs. *Flexible Services and Manufacturing Journal, 33*(1), 43–106.

Elmi, Z., Singh, P., Meriga, V. K., Goniewicz, K., Borowska-Stefańska, M., Wiśniewski, S., & Dulebenets, M. A. (2022). Uncertainties in liner shipping and ship schedule recovery: A state-of-the-art review. *Journal of Marine Science and Engineering, 10*(5), 563.

Halvorsen-Weare, E. E., Fagerholt, K., & Rönnqvist, M. (2013). Vessel routing and scheduling under uncertainty in the liquefied natural gas business. *Computers & Industrial Engineering, 64*(1), 290–301.

ICE Cargo. 2021, September 17. How bad weather impacts shipping (and how to deal with it). Available at: https://www.icecargo.com.au/weather-impacts-shipping/ (Accessed: 12 June 2022).

Jones, D. A., Farkas, J. L., Bernstein, O., Davis, C. E., Turk, A., Turnquist, M. A., … Sawaya, W. (2011). US import/export container flow modeling and disruption analysis. *Research in Transportation Economics, 32*(1), 3–14.

G. Kay Hurricane Ida aftermath will worsen supply chain bottlenecks and lead to even more shortages and price hikes, experts warn https://www.businessinsider.com/hurricane-ida-aftermath-will-worsen-supply-chain-disaster-experts-warn-2021-9 2021 Available at: Accessed: 12 June 2022.

Kontovas, C. (2014). The green ship routing and scheduling problem (GSRSP): A conceptual approach. *Transportation Research Part D: Transport and Environment, 31*, 61–69.

Li, C., Qi, X., & Lee, C. Y. (2015). Disruption recovery for a vessel in liner shipping. *Transportation Science, 49*(4), 900–921.

Li, C., Qi, X., & Song, D. (2016). Real-time schedule recovery in liner shipping service with regular uncertainties and disruption events. *Transportation Research Part B: Methodological, 93*, 762–788.

J. Lim Malaysian floods disrupt semiconductor supply chain; devastates workers, Tech Wire Asia https://techwireasia.com/2021/12/malaysian-floods-devastate-workers-disrupts-semiconductor-supply-chain/ 2021 Available at: Accessed: 17 October 2022.

Liu, B., Li, Z. C., Wang, Y., & Sheng, D. (2021). Short-term berth planning and ship scheduling for a busy seaport with channel restrictions. *Transportation Research Part E: Logistics and Transportation Review, 154*, Article 102467.

Liu, M., Liu, X., Chu, F., Zhu, M., & Zheng, F. (2020). Liner ship bunkering and sailing speed planning with uncertain demand. *Computational and Applied Mathematics, 39*(1), 1–23.

Ma, W., Zhang, J., Han, Y., Zheng, H., Ma, D., & Chen, M. (2022). A chaos-coupled multi-objective scheduling decision method for liner shipping based on the NSGA-III algorithm. *Computers & Industrial Engineering, 174*, Article 108732.

Marla, L., Vaaben, B., & Barnhart, C. (2017). Integrated disruption management and flight planning to trade off delays and fuel burn. *Transportation Science, 51*(1), 88–111.

G. Marle One apus stack collapse losses expected to top $200m, The Loadstar https://theloadstar.com/one-apus-stack-collapse-losses-expected-to-top-200m/ 2022 Available at: Accessed: 17 October 2022.

Mavrotas, G. (2009). Effective implementation of the ε-constraint method in multi-objective mathematical programming problems. *Applied Mathematics and Computation, 213*(2), 455–465.

McLean, C. (2021). *Government action and the new blue economy. In Preparing a Workforce for the New Blue Economy* (pp. 513–525). Elsevier.

Mehrzadegan, E., Ghandehari, M., & Ketabi, S. (2022). A joint dynamic inventory-slot allocation model for liner shipping using revenue management concepts. *Computers & Industrial Engineering, 170*, Article 108333.

Meng, Q., Wang, S., Andersson, H., & Thun, K. (2014). Containership routing and scheduling in liner shipping: Overview and future research directions. *Transportation Science, 48*(2), 265–280.

Menhat, M., Zaideen, I. M. M., Yusuf, Y., Salleh, N. H. M., Zamri, M. A., & Jeevan, J. (2021). The impact of Covid-19 pandemic: A review on maritime sectors in Malaysia. *Ocean & Coastal Management, 209*, Article 105638.

Mulder, J., & Dekker, R. (2019). Designing robust liner shipping schedules: Optimizing recovery actions and buffer times. *European Journal of Operational Research, 272*(1), 132–146.

Mulder, J., van Jaarsveld, W., & Dekker, R. (2019). Simultaneous optimization of speed and buffer times with an application to liner shipping. *Transportation Science, 53*(2), 365–382.

Oyenuga, A. (2021). Perspectives on the impact of the COVID-19 pandemic on the global and African maritime transport sectors, and the potential implications for Africa's maritime governance. *WMU Journal of Maritime Affairs, 20*(2), 215–245.

Pasha, J., Dulebenets, M. A., Fathollahi-Fard, A. M., Tian, G., Lau, Y. Y., Singh, P., & Liang, B. (2021). An integrated optimization method for tactical-level planning in liner shipping with heterogeneous ship fleet and environmental considerations. *Advanced Engineering Informatics, 48*, Article 101299.

Pasha, J., Dulebenets, M. A., Kavoosi, M., Abioye, O. F., Theophilus, O., Wang, H., … Guo, W. (2020). Holistic tactical-level planning in liner shipping: An exact optimization approach. *Journal of Shipping and Trade, 5*(1), 1–35.

Paul, J. A., & Maloni, M. J. (2010). Modeling the effects of port disasters. *Maritime Economics & Logistics, 12*(2), 127–146.

PBT International Oil price information https://pbt-international.com/price-information/ 2022 Available at: Accessed: 12 June 2022.

Ports.com, 2022. Sea routes and distances. Available at: http://ports.com/sea-route/ (Accessed: 18 October 2022).

Qi, X. (2015). *Disruption management for liner shipping. In Handbook of ocean container transport logistics* (pp. 231–249). Cham: Springer.

Sun, H., Lam, J. S. L., & Zeng, Q. (2021). The dual-channel sales strategy of liner slots considering shipping e-commerce platforms. *Computers & Industrial Engineering, 159*, Article 107516.

Tierney, K., Ehmke, J. F., Campbell, A. M., & Müller, D. (2019). Liner shipping single service design problem with arrival time service levels. *Flexible Services and Manufacturing Journal, 31*(3), 620–652.

UNCTAD Review of Maritime Transport 2021 - overview - UNCTAD https://unctad.org/system/files/official-document/rmt2021summary_en.pdf 2021 Available at: Accessed: October 18 2022.

Wang, S., & Meng, Q. (2012a). Robust schedule design for liner shipping services. *Transportation Research Part E: Logistics and Transportation Review, 48*(6), 1093–1106.

Wang, S., & Meng, Q. (2012b). Sailing speed optimization for container ships in a liner shipping network. *Transportation Research Part E: Logistics and Transportation Review, 48*(3), 701–714.

Wang, S., Alharbi, A., & Davy, P. (2014). Liner ship route schedule design with port time windows. *Transportation Research Part C: Emerging Technologies, 41*, 1–17.

Wang, Y., & Wang, S. (2021). Deploying, scheduling, and sequencing heterogeneous vessels in a liner container shipping route. *Transportation Research Part E: Logistics and Transportation Review, 151*, Article 102365.

Wang, S., Meng, Q., & Liu, Z. (2013). Bunker consumption optimization methods in shipping: A critical review and extensions. *Transportation Research Part E: Logistics and Transportation Review, 53*, 49–62.

Xing, J., & Wang, Y. (2019). In *Disruption Management in Liner Shipping: A Service-Cost Trade-off Model for Vessel Schedule Recovery Problem* (pp. 794–799). IEEE.

Xu, L., Yang, S., Chen, J., & Shi, J. (2021). The effect of COVID-19 pandemic on port performance: Evidence from China. *Ocean & Coastal Management, 209*, Article 105660.

Yu, G., & Qi, X. (2004). *Disruption management: Framework, models and applications*. World Scientific.

Zhao, X., Lin, Q., & Yu, H. (2019). An improved mathematical model for green lock scheduling problem of the Three Gorges Dam. *Sustainability, 11*(9), 2640.

Zheng, J., Ma, Y., Ji, X., & Chen, J. (2021). Is the weekly service frequency constraint tight when optimizing ship speeds and fleet size for a liner shipping service? *Ocean & Coastal Management, 212*, Article 105815.

Zheng, J., Yang, L., Ni, L., Fagerholt, K., & Zhang, Y. (2022). Efficient models for the liner shipping hub location problem with spatial structure. *Computers & Industrial Engineering, 173*, Article 108725.